Available online at www.sciencedirect.com
SCIENCE DIRECT®
Biochemical and Biophysical Research Communications 323 (2004) 491–498
BBRC
www.elsevier.com/locate/ybbrc

MD-2 is required for the full responsiveness of mast cells to LPS but not to PGN

Hiroko Ushio[a,*], Atsuhito Nakao[a], Volaluck Supajatura[e], Kensuke Miyake[d], Ko Okumura[a,b], Hideoki Ogawa[a,c]

[a] *Atopy (Allergy) Research Center, Juntendo University, School of Medicine, 2-1-1 Hongo, Bunkyo-ku, Tokyo 113-8421, Japan*
[b] *Department of Immunology, Juntendo University, School of Medicine, 2-1-1 Hongo, Bunkyo-ku, Tokyo 113-8421, Japan*
[c] *Department of Dermatology, Juntendo University, School of Medicine, 2-1-1 Hongo, Bunkyo-ku, Tokyo 113-8421, Japan*
[d] *Division of infectious Genetics, Department of Microbiology and Immunology, The Institute of Medical Science, The University of Tokyo, 4-6-1 Shirokanedai, Tokyo 108-8639, Japan*
[e] *Department of Microbiology, Faculty of Medicine, Chiang Mai University, Chiang Mai 50200, Thailand*

Received 21 July 2004

Abstract

To address the role played by MD-2 in mast cell recognition of LPS, we examined bone marrow-derived mast cells (BMMCs) from MD-2 gene-targeted mice. BMMCs from MD-2−/− mice showed impaired cytokine production (TNF-α, IL-6, IL-13, and IL-1β) in response to LPS from *Escherichia coli*, but not to peptidoglycan (PGN) from *Staphylococcus aureus*. In a mast cell-dependent acute septic model, MD-2 deficiency of mast cell resulted in significantly higher mortality due to defective neutrophil recruitment and the production of cytokines in the peritoneal cavity, which was similar to mice with TLR4-deficient mast cells. The TLR2-dependent activation of skin mast cells by PGN was not altered by the absence of MD-2 in vivo. Collectively, MD-2 is essential for the recognition of LPS by TLR4 but not for that of PGN by TLR2 of mast cells.

Keywords: Mast cells/basophils; Toll-like receptor; MD-2; Bacterial; Rodent; Lipopolysaccharide

Mast cells are primarily known as effector cells of allergic diseases and chronic inflammatory responses. However, recent accumulating evidence has shown that mast cells play an important role in host defense against bacterial infection [1–4]. Innate immune responses elicited by mast cells also rely on the ability of the cells to recognize the molecular motifs of microorganisms through pattern recognition receptors called toll-like receptors (TLR). A wide variety of bacterial components including LPS, peptidoglycan (PGN), lipoteichoic acid (LTA), lipoarabinomannan, lipopeptides, and bacterial DNA are capable of stimulating the innate immune system through specific TLR [5–7]. However, the precise mechanisms for the recognition of each ligand by respective TLR are complex and poorly understood.

LPS from gram-negative bacteria is among the best-characterized ligands for TLR4. The lipid A portion of LPS is conserved among gram-negative bacteria and appears to be responsible for the biological toxicity of LPS [8,9]. At least four cellular proteins are known to participate in LPS recognition and cellular activation, LPS-binding protein (LBP), CD14, TLR4, and MD-2 [6,7,10,11]. The plasma protein, LBP, dramatically accelerates the binding of monomer LPS to CD14, which usually forms aggregates in aqueous environments, thereby enhancing the sensitivity of cells to

* Corresponding author. Fax: +81 3 3813 5512.
E-mail address: hushio@med.juntendo.ac.jp (H. Ushio).

0006-291X/$ - see front matter © 2004 Elsevier Inc. All rights reserved.
doi:10.1016/j.bbrc.2004.08.108

LPS [12,13]. CD14 is a glycosylphosphatidylinositol (GPI)-linked cell surface protein that serves as the major LPS receptor but is itself devoid of signaling [14]. Experiments using TLR4 gene-targeted mice or TLR4-mutated C3H/HeJ mice have shown that TLR4 is a signal transducer of cell activation via LPS [15,16]. MD-2 was cloned through its homology with MD-1 that associates with and is required for the signaling and surface expression of RP105, a leucine-rich-repeat-containing protein similar to TLRs [17–19]. Since MD-2 lacks a transmembrane domain, it associates with the cell through its interaction with the extracellular domain of TLR4. Evidence that both TLR4 and MD-2 participate directly in the discrimination of LPS structures has been demonstrated using mutated MD-2 lacking one or two N-glycosylation sites [20–22]. Also, da Silva et al. [23] observed that direct physical contact occurs between LPS and CD14-TLR4–MD2. Thus, the physical association of MD-2 with TLR4 is critical for LPS recognition by TLR4. Furthermore, it has been shown that MD-2 is important for the correct distribution of TLR4 on the surface of cells such as MD-1, which also plays an important role in the surface expression of RP105 on B cells [18,24]. Thus, it appears that MD-2 is an indispensable molecule in the LPS-sensing complex.

We have previously demonstrated that mouse mast cells express TLR4 and are activated by LPS through that [3,4]. However, the roles played by MD-2 in mast cells for both LPS recognition and TLR4 distribution remain unclear. In this study, we demonstrate that MD-2 is required for the full responsiveness of mast cells against LPS but not PGN. We also demonstrate that MD-2, as well as the TLR4 molecule, plays a crucial role in the recognition and activation of peritoneal mast cells in acute septic bacteria infection.

Methods

Mice. MD-2-deficient (MD-2−/−) and heterozygous (MD-2+/−) mice were kindly provided by Dr. K. Miyake of Tokyo University, Japan [24]. We used MD-2+/− mice as control mice since no phenotypic difference was observed between MD-2+/− and MD-2+/+ mice. TLR4-deficient (TLR4−/−) or TLR2-deficient (TLR2−/−) mice were kindly provided by Dr. S. Akira of Osaka University, Japan [15,25]. WBB6F$_1$-W/W^v mice were purchased from Japan SLC (Hamamatsu, Japan). All animal experiments were performed under the approval of the Institutional Review Board of Juntendo University.

Generation of bone marrow-derived mast cells. Bone marrow-derived mast cells (BMMCs) were generated from the femoral bone marrow cells of mice and maintained in the presence of 10% pokeweed mitogen-stimulated spleen-conditioned medium (PWM-SCM) as a source of mast cell growth factors as previously described [3,4]. After 4 weeks of culture, more than 98% of cells were identifiable as mast cells as determined by toluidine blue staining and FACS analysis of cell surface expressions of both *c-kit* and FcεRI.

RT-PCR analysis of the mRNA expression of TLR and MD-2. Total RNA was extracted from BMMCs using STAT-60 (Tel-Test, Friendswood, TX) according to the manufacturer's instructions. First-strand cDNA was constructed from 3 μg of total RNA with oligo(dT)$_{12-18}$ as the primer using Superscript II RNase H$^-$ reverse transcriptase (Life Technologies, Rockville, MD). PCR was performed using specific primers for mouse MD-2 (5′-ATG TTG CCA TTT ATT CTC TTT TCG ACG-3′ and 5′-ATT GAC ATC ACG GCG GTG AAT GAT G-3′) and for mouse TLR4 (AF110133) [26] and mouse GAPDH (5′-AGT ATG ACT CCA CTC ACG GCA A-3′ and 5′-TGT CGC TCC TGG AAG ATG GT-3′).

FACS analysis. Single cell suspensions were incubated at 2×10^5 cells/100 μl in staining buffer (PBS containing 0.5% BSA and 0.01% NaN_3) with anti-TLR4–MD-2 (MTS510: Hycult Biotechnology, PB Uden, The Netherlands), followed by FITC-rabbit F (ab′)$_2$ anti-rat IgG (ICN Pharmaceuticals, Aurora, OH) or mouse IgE Ab (BD Biosciences, San Jose, CA), followed by FITC-anti-mouse IgE (BD Biosciences, San Jose, CA), or FITC-anti-*c*-kit Ab (BD Biosciences, San Jose, CA). Flow cytometric analysis was performed using FACS caliber (BD Biosciences, San Jose, CA).

Measurement of cytokine concentrations. BMMCs (2×10^6 cells/ml) in complete culture medium were stimulated with the indicated concentration of LPS from *Escherichia coli* (serotype 0111:B4; Sigma–Aldrich) or PGN from *Staphylococcus aureus* (Sigma–Aldrich) in the presence of 10% FCS and PWM-SCM. For IgE-mediated stimulation, BMMCs (5×10^5/ml) were incubated with 1 μg of anti-TNP mouse IgE (BD Biosciences, San Jose, CA) on ice for 2 h. After washing of the cells twice, BMMCs (2×10^6 cells/ml) in complete culture medium were stimulated with 250 ng/ml of anti-mouse IgE (BD Biosciences, San Jose, CA). Cells were incubated at 37 °C, 3 h for TNF-α or 6 h for IL-1β, IL-6, and IL-13. The amount of each cytokine in the supernatant was measured by ELISA kit (Genzyme Techne, Minneapolis, MN, USA).

Reconstitution of W/W^v mice with BMMCs. Mast cell-deficiency of W/W^v mice in the peritoneal cavity was selectively reconstituted by injecting 2×10^6 BMMCs from MD-2+/−, MD-2−/− or TLR4−/−, mice into the peritoneal cavity as previously described [3,4]. The reconstitution of the skin mast cells of W/W^v mice was performed using an intradermal injection of 1×10^6 BMMCs from MD-2+/−, MD-2−/−, TLR4−/−, or TLR2−/− mice [27,28]. Five weeks after injection of BMMCs, the mice were used for experiments. Reconstitution of the mast cells was confirmed by toluidine blue or alcian blue/safranin staining of the cytospun preparation of peritoneal cells or formalin-fixed tissue section of the skin.

Cecal ligation and puncture. Cecal ligation and puncture (CLP) was performed as previously described [3]. Briefly, mice were anesthetized and the cecum was ligated with 4–0 silk and punctured using a 21-gauge needle. After CLP, mice were observed for mortality over a period of 10 days.

Differential cell counts and estimation of cytokine concentrations in peritoneal exudates. Peritoneal exudates were collected 6 h after CLP induction. The total cell number was counted, and the differential cell count of infiltrating leukocytes was performed by counting 500 leukocytes under an oil immersion field after staining cytospun preparations with Diff-Quik (International Reagents, Kobe, Japan). The amount of each cytokine in the peritoneal fluid was determined by ELISA as described above.

Induction of skin inflammation. PGN-induced skin inflammation was performed as previously described [4]. Mice were intradermally injected with 20 μl PGN (100 μg/ml in saline) or saline into each ear. For the PCA reaction, anti-TNP IgE (25 μg in 20 μl) was injected intradermally into the ears 2 h before Ag (TNP-BSA) application. Vascular leakage was visualized by an intravenous injection of 0.5% Evans blue (0.25 ml) 5 min before PGN or antigen application. Thirty minutes after the application of PGN or the antigen, the ears were removed and the amount of dye in the ear was measured as previously described [4]. The amount of dye was calculated according to the standard curve of known concentration of Evans blue.

Statistical analysis. Statistical analysis was performed using Student's *t* test. Statistical analysis of survival data in the CLP experiment was performed using the Log-rank test.

Results

Expression of the MD-2 transcript in BMMCs

To address the role played by MD-2 in the activation of mast cells by gram-negative bacteria-derived LPS, we generated BMMCs from MD-2 gene-targeted mice. The mRNA and protein expression of MD-2 in BMMCs was investigated by RT-PCR and FACS analysis using anti-TLR4 mAb (MTS510), which specifically detects the TLR4–MD-2 complex [29]. Although TLR4 mRNA was present in BMMCs from MD-2+/– or MD-2–/– mice (Fig. 1A), the TLR4–MD-2 complex was not expressed on BMMCs from MD-2–/– mice (Fig. 1B), demonstrating the absence of MD-2 protein on the cell surface. TLR4–/– mice also did not express TLR4–MD-2 detected by MTS510, due to the absence of TLR4, although the amount of mRNA expression of MD-2 in TLR4–/– mice was not altered in the absence of TLR4 (Figs. 1A and B). The expressions of other surface molecules, such as the *c-kit* or IgE receptor, were not different between the BMMCs of these mice (Fig. 1B).

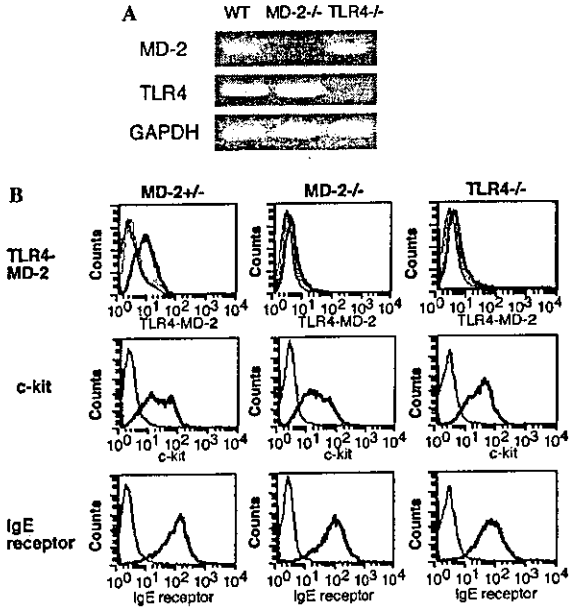

Fig. 1. Expression of the MD-2 molecule of mast cells. (A) BMMCs were prepared from MD-2+/–, MD-2–/–, or TLR4–/– mice and used for RT-PCR analysis to detect the mRNA of MD-2, TLR4 and GAPDH. (B) BMMCs from MD-2+/–, MD-2–/–, or TLR4–/– mice were stained with mAbs to TLR4-MD-2 (MTS510), followed by FITC-anti-rat IgG, or mouse IgE, followed by FITC-anti-mouse IgE or FITC labeled anti-*c*-kit Abs. The solid line shows staining with isotype-matched Ab; the dotted line shows isotype-matched Ab and the second Ab alone. The bold line shows staining with respective specific Abs and the second Ab.

Requirement of MD-2 for the full responsiveness of BMMCs to LPS but not to PGN in vitro

As we have previously reported that LPS induced the secretion of inflammatory cytokines (TNF-α, IL-1β, IL-6, and IL-13) from the BMMCs in a TLR4-dependent manner [3,4], we examined the LPS responsiveness of BMMCs of MD-2–/– mice by stimulation with increasing concentrations of LPS (from *E. coli*) or PGN (from *S. aureus*). LPS induced the secretion of these cytokines from the BMMCs of MD-2+/– mice, but not from those of MD-2–/– or TLR4–/– mice (Fig. 2A). In contrast, there were no significant differences in TNF-α, IL-6, and IL-13 secretion by the BMMCs of MD-2+/–, MD-2–/–, and TLR4–/– mice when stimulated with PGN (a TLR2 ligand) or with IgE receptor cross-linking (Figs. 2A and B). PGN or IgE receptor cross-linking did not lead to detectable levels of IL-1β secretion in any BMMCs as has been reported [4]. Consistent with previous data, LPS did not induce the degranulation of mast cells of any mice (MD-2+/–, MD-2–/–, and TLR4–/–), although there were no differences in the ability of these BMMCs to degranulate upon IgE receptor cross-linking when evaluated by β-hexosaminidase release (data not shown).

Requirement of MD-2 of mast cells for host-innate immune response against gram-negative bacteria infection

To address the roles played by mast cell-MD-2 in bacterial infection in vivo, we used an acute septic peritonitis model in which host protection against bacteria was known to depend on mast cells in the peritoneal cavity. Peritoneal mast cells of mast cell-deficient W/W^v mice were reconstituted with BMMCs from MD-2+/–, MD-2–/– or TLR4–/– mice and subjected to CLP. Five weeks after reconstitution, there were no significant differences in the number of peritoneal mast cells between W/W^v mice reconstituted with different BMMCs (MD2+/–, MD-2–/–, and TLR4–/–: $4.45 \pm 0.64 \times 10^4$, $5.43 \pm 1.12 \times 10^4$, and $5.41 \pm 1.16 \times 10^4$ cell per mouse, respectively). More than 95% of these mast cells showed positive staining with alcian blue/safranin that was the property of connective tissue-type mast cells (data not shown). Consistent with previous reports [3,4], mast cell-deficient W/W^v mice all died within 3 days after CLP induction (Fig. 3A). In contrast, the reconstitution of W/W^v mice with BMMCs from MD-2+/– mice protected the host from acute peritonitis-induced death ($p < 0.001$ vs W/W^v) (Fig. 3A). Similar reconstitution of W/W^v mice with

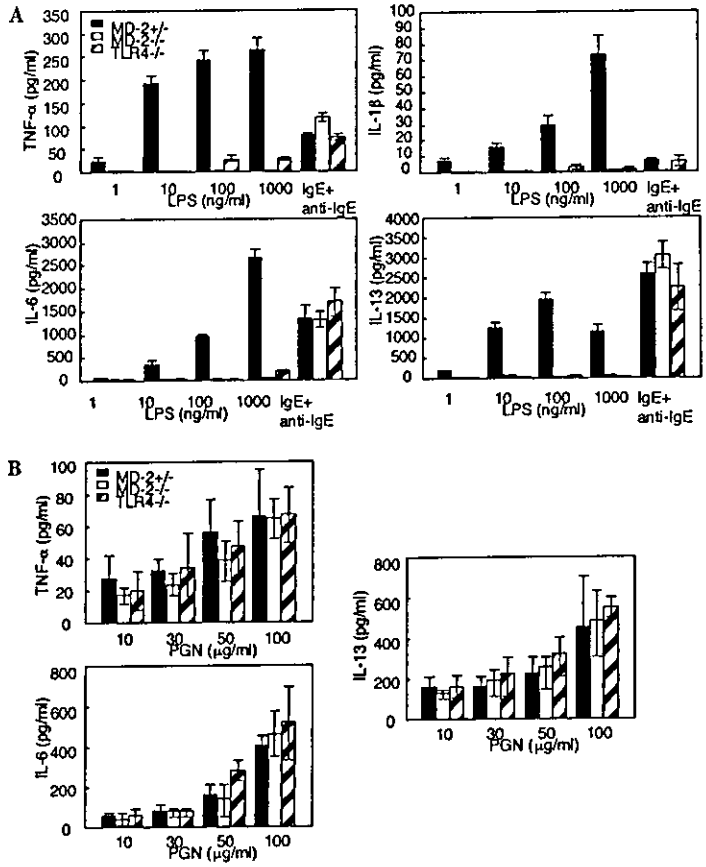

Fig. 2. MD-2 is required for the activation of BMMCs by LPS. BMMCs from MD-2+/– (filled bars), MD-2–/– (open bars), or TLR4–/– (striped bars) were stimulated with the indicated concentrations of LPS (A) or PGN (B), 3 h for TNF-α and 6 h for other cytokines. For IgE receptor-mediated stimulation, BMMCs were sensitized with IgE and challenged with anti-IgE as described in Methods. The cytokine concentrations in the supernatant were determined as described in Methods. Data shown are means ± SD of three to four experiments conducted with different BMMC preparations.

BMMCs from MD-2–/– or TLR4–/– slightly improved the survival rate, but the rate was significantly lower than that of W/W^v mice reconstituted with MD-2+/– BMMCs ($p < 0.05$) (Fig. 3A). The survival rate of W//W^v mice with MD-2+/– BMMCs was not significantly different from that of W//W^v mice with WBB6F$_1$-+/+ BMMCs (data not shown). These results indicate again that mast cells play an important role in host protection from early enterobacterial infection via MD-2 in addition to the TLR4 molecule.

As a previous study suggested that defective production of TNF-α and early recruitment of neutrophils in the absence of mast cell are responsible for host protection from acute septic peritonitis-induced death [2], we investigated whether defective leukocyte recruitment in the peritoneal cavity after CLP was associated with MD-2 deficiency of mast cell. When we examined the number of infiltrating cells and the amount of inflammatory cytokines in the peritoneal cavity, W/W^v mice without mast cell or with MD-2/TLR4-deficient mast cells showed significantly lower levels of cytokine and neutrophil infiltration 6 h after CLP than those with intact mast cells ($p < 0.01$) (Figs. 3B and C). Thus, early leukocyte, especially neutrophil recruitment into the peritoneal cavity by the production of inflammatory cytokines was highly dependent on mast cell activation by enterobacteria via MD-2/TLR4 and was one of the crucial factors to protect the host from acute septic peritonitis-induced death. These results indicate that MD-2, as well as the TLR4 molecule, plays an important role in mast cell activation by enterobacteria infection in vivo.

MD-2 deficiency did not affect TLR2 of mast cell-dependent acute skin response

To verify the roles played by MD-2 in the TLR2-dependent activation of skin mast cells by PGN in vivo, we compared the responses elicited by an intradermal injection of PGN into the ear of W/W^v mice and W/W^v mice reconstituted with BMMCs from MD-2+/–, MD-2–/–,

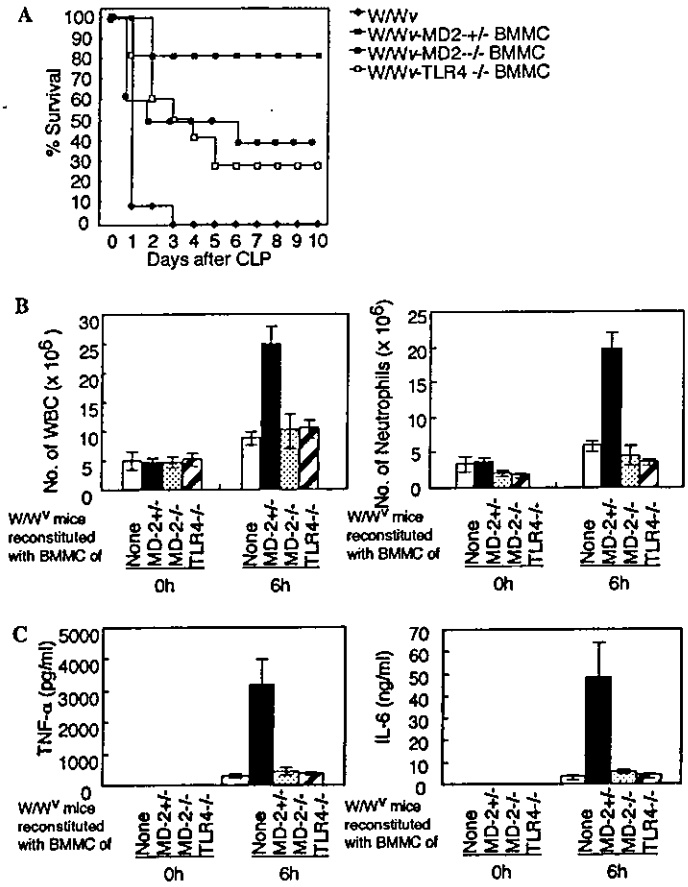

Fig. 3. Both MD-2 and TLR4 of mast cells are required for the full expression of innate immunity in a mast cell-dependent sepsis model. (A) W/W^v mice without reconstitution (♦) or reconstitution with BMMCs from MD-2+/– (■), MD-2–/– (●) or TLR4–/– (□) mice (10 mice/group) underwent CLP. The mortality was observed and expressed as percent survival. (B) Six hours after CLP, total numbers of leukocytes and neutrophils in the peritoneal cavity were estimated by differential cell count and expressed as total cells/mouse. (C) The levels of individual cytokines were measured by ELISA. Data shown are means ± SD of four mice.

TLR4–/–, or TLR2–/– mice. Vascular permeability, evaluated by the extravasation of Evans blue dye, was significantly increased by PGN ($p < 0.001$) in wild-type mice but not in mast cell-deficient W/W^v, suggesting that this reaction was dependent on mast cells in the skin (Fig. 4). The reconstitution of skin mast cells of W/W^v mice with BMMCs from MD-2+/–, MD-2–/–, and TLR4–/– but not from TLR2–/– mice resulted in increased extravasation of the dye, indicating that the deficiency of MD-2 as well as TLR4 in skin mast cells did not confer the TLR2-mediated skin inflammation by PGN even in vivo. Consistent with the previous data [4], LPS did not cause severe vasodilatation as much as PGN within 30 min (data not shown). The number of skin mast cells 5 weeks after the reconstitution of each BMMC was not different between these mice (data not shown). Also, there were no differences in the functional ability of reconstituted and differentiated mast cells to degranulate in response to IgE receptor-mediated activation (Fig. 4). Thus, unlike CD14, which seems to bind soluble PGN from *S. aureus* and lipoarabinomannan from *Mycobacterium* [30], MD-2 associated with TLR4 directly interprets LPS structures and does not confer the responsiveness of the TLR2 ligand.

Discussions

The roles played by MD-2 in the activation of mast cells by gram-negative bacteria-derived LPS were examined both in vitro and in vivo. We generated BMMCs from MD-2–/– mice as well as MD-2+/– and TLR4–/– mice. There were no differences in the growth rate between these mast cells during the course of experiment. Also the properties of mast cells evaluated by the expression of the *c-kit* and IgE receptor were not different between these mast cells (Fig. 1B). The importance of MD-2 in LPS responsiveness has been implicated in

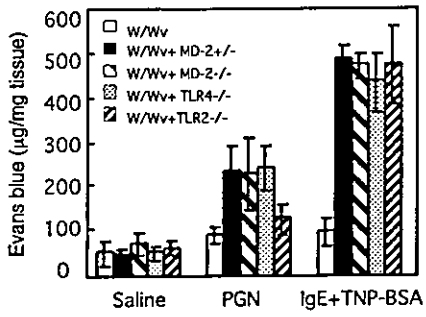

Fig. 4. PGN-TLR2 activation of skin mast cell is not affected by the absence of MD-2. Skin mast cells of W/W^v mice without reconstitution (□) or reconstituted with BMMCs from MD-2+/− (■), MD-2−/− (▨), TLR4−/− (▤) or TLR2−/− (▨) mice were intravenously injected with 0.5% of Evans blue 5 min before intradermal administration (20 μl) of PGN (100 μg/ml) to the ears. The dye content in the tissues was measured 30 min after PGN administration as described in Methods. The concentration of dye content in the tissues by IgE-mediated stimulation was measured as described in Methods. Data shown are means ± SD of three mice.

both LPS recognition and the proper surface distribution of TLR4 [24]. It has been reported that an association between MD-2 and TLR4 occurs in the endoplasmic reticulum (ER) in which the endoplasmic reticulum chaperone gp96 plays an important role [31]. Thus, it is generally thought that the distribution of TLR4 alone in the Golgi apparatus does not necessarily lead to LPS recognition and signaling. Although, there is an exception of intestinal epithelial cells, in which LPS recognition occurs in the Golgi apparatus after LPS internalization [32]. The result that MD-2-deficient mast cell could not respond against LPS in vitro and in vivo, suggesting that TLR4 alone in the Golgi apparatus may not be enough to recognize LPS and signal in the mast cells. An approach using a mutated form of MD-2 by replacing Cys95 with Tyr95, which abolishes the LPS responses but not the cell surface expression of TLR4 [20–22], will help to clarify this point.

Also, our in vivo results indicate that soluble forms of MD-2 which might circulate in the serum [33,34] did not confer or restore the responsiveness of peritoneal mast cells against gram-negative bacteria. Although an in vitro experiment has shown that soluble MD-2 as low as 50 pM can rescue the hypo-responsiveness of cells to LPS [33,34], little is known about the physiological role of soluble MD-2 in vivo. As serum concentrations of soluble MD-2 have never been determined, but are probably below 50 pM, the concentrations of circulating MD-2 in vivo may not be sufficient to induce the responsiveness of peritoneal mast cells against bacteria-derived LPS in our experimental system.

Unlike CD14, which is implicated in the recognition of ligands for both TLR4 and TLR2 [30], it seems that MD-2 is required only for the recognition and binding of TLR4 ligand. In contrast to the observation that TLR2-associated MD-2 enhances the cell responsiveness against several TLR2 ligands including PGN [35], we could not observe any defect in the TLR2-mediated mast cell activation in MD-2-deficient mice. These discrepancies may arise from differences in the species (human vs mouse), or the cells used (artificially transfected-HEK293 vs naturally developed-mast cell).

It has been demonstrated that MD-2 is required for the recognition of various TLR4 ligands other than LPS, such as Taxol [36], HSP60 [37], and extra domain A of fibronectin [38]. We confirmed that BMMCs could be activated by extra domain A of fibronectin in a TLR4-dependent manner (manuscript in preparation), it would be interesting to examine how these structurally different molecules are recognized by MD-2/TLR4 in mast cells.

In the CLP model, a slight improvement of the survival rate in W/W^v mice reconstituted with BMMCs from MD-2−/− or TLR4−/− was observed but was not significantly different from W/W^v mice without receiving mast cell reconstitution. The exact reason for this improvement was not clear from this experiment. It is possible that other molecules than TLR4/MD-2 on mast cells, such as CD48 and complement receptor, may confer the activation of mast cells by enterobacteria infection as has been reported [39,40].

Taken together, this study first shows in vivo that MD-2 is essential for the full responsiveness of mast cells against LPS but not PGN, a TLR2 ligand. Also, this study shows that in vivo circulating forms of MD-2 may not be enough to rescue the responsiveness of reconstituted-mast cells against enterobacteria. To generalize the requirement of both TLR4 and MD-2 molecules for the proper distribution of TLR4 on the surface of cells, a careful examination of TLR4 distribution in mast cells in the absence of MD-2 is required (under investigation). The clarification of the mechanism of mast cell activation by microorganisms through these receptors would be helpful to understand the physiological roles played by mast cells in innate immune responses.

Acknowledgments

This work was supported in part by a grant from the Ministry of Education, Culture, Sports, Science and Technology, Japan. The authors thank Dr. S. Akira for the generous gift of TLR4- and TLR2-deficient mice. We also thank the staff of the Atopy Research Center for fruitful discussions and technical assistance.

References

[1] S.J. Galli, B.K. Wershil, The two faces of the mast cell, Nature 381 (1996) 21–22.

[2] R. Malaviya, T. Ikeda, E. Ross, S.N. Abraham, Mast cell modulation of neutrophil influx and bacterial clearance at sites of infection through TNF-alpha, Nature 381 (1996) 77–80.
[3] V. Supajatura, H. Ushio, A. Nakao, K. Okumura, C. Ra, H. Ogawa, Protective roles of mast cells against enterobacterial infection are mediated by Toll-like receptor 4, J. Immunol. 167 (2001) 2250–2256.
[4] V. Supajatura, H. Ushio, A. Nakao, S. Akira, K. Okumura, C. Ra, H. Ogawa, Differential responses of mast cell Toll-like receptors 2 and 4 in allergy and innate immunity, J. Clin. Invest. 109 (2002) 1351–1359.
[5] S. Akira, K. Takeda, T. Kaisho, Toll-like receptors: critical proteins linking innate and acquired immunity, Nat. Immunol. 2 (2001) 675–680.
[6] A. Aderem, R.J. Ulevitch, Toll-like receptors in the induction of the innate immune response, Nature 406 (2000) 782–787.
[7] D.M. Underhill, A. Ozinsky, Toll-like receptors: key mediators of microbe detection, Curr. Opin. Immunol. 14 (2002) 103–110.
[8] M.G. Netea, M. van Deuren, B.J. Kullberg, J.M. Cavaillon, J.W. Van der Meer, Does the shape of lipid A determine the interaction of LPS with Toll-like receptors?, Trends Immunol. 23 (2002) 135–139.
[9] A.M. Hajjar, R.K. Ernst, J.H. Tsai, C.B. Wilson, S.I. Miller, Human Toll-like receptor 4 recognizes host-specific LPS modifications, Nat. Immunol. 3 (2002) 354–359.
[10] S. Akira, Mammalian Toll-like receptors, Curr. Opin. Immunol. 15 (2003) 238.
[11] K. Miyake, Innate recognition of lipopolysaccharide by CD14 and toll-like receptor 4-MD-2: unique roles for MD-2, Int. Immunopharmacol. 3 (2003) 119–128.
[12] E. Hailman, H.S. Lichenstein, M.M. Wurfel, D.S. Miller, D.A. Johnson, M. Kelley, L.A. Busse, M.M. Zukowski, S.D. Wright, Lipopolysaccharide (LPS)-binding protein accelerates the binding of LPS to CD14, J. Exp. Med. 179 (1994) 269–277.
[13] M.J. Fenton, D.T. Golenbock, LPS-binding proteins and receptors, J. Leukoc. Biol. 64 (1998) 25–32.
[14] S.D. Wright, R.A. Ramos, P.S. Tobias, R.J. Ulevitch, J.C. Mathison, CD14, a receptor for complexes of lipopolysaccharide (LPS) and LPS binding protein, Science 249 (1990) 1431–1433.
[15] K. Hoshino, O. Takeuchi, T. Kawai, H. Sanjo, T. Ogawa, Y. Takeda, K. Takeda, S. Akira, Cutting edge: Toll-like receptor 4 (TLR4)-deficient mice are hyporesponsive to lipopolysaccharide: evidence for TLR4 as the Lps gene product, J. Immunol. 162 (1999) 3749–3752.
[16] A. Poltorak, X. He, I. Smirnova, M.Y. Liu, C. Van Huffel, X. Du, D. Birdwell, E. Alejos, M. Silva, C. Galanos, M. Freudenberg, P. Ricciardi-Castagnoli, B. Layton, B. Beutler, Defective LPS signaling in C3H/HeJ and C57BL/10ScCr mice: mutations in Tlr4 gene, Science 282 (1998) 2085–2088.
[17] R. Shimazu, S. Akashi, H. Ogata, Y. Nagai, K. Fukudome, K. Miyake, M. Kimoto, MD-2, a molecule that confers lipopolysaccharide responsiveness on Toll-like receptor 4, J. Exp. Med. 189 (1999) 1777–1782.
[18] Y. Nagai, R. Shimazu, H. Ogata, S. Akashi, K. Sudo, H. Yamasaki, S. Hayashi, Y. Iwakura, M. Kimoto, K. Miyake, Requirement for MD-1 in cell surface expression of RP105/CD180 and B-cell responsiveness to lipopolysaccharide, Blood 99 (2002) 1699–1705.
[19] Y. Miura, R. Shimazu, K. Miyake, S. Akashi, H. Ogata, Y. Yamashita, Y. Narisawa, M. Kimoto, RP105 is associated with MD-1 and transmits an activation signal in human B cells, Blood 92 (1998) 2815–2822.
[20] J. da Silva Correia, R.J. Ulevitch, MD-2 and TLR4 N-linked glycosylations are important for a functional lipopolysaccharide receptor, J. Biol. Chem. 277 (2002) 1845–1854.
[21] S. Viriyakosol, T. Kirkland, K. Soldau, P. Tobias, MD-2 binds to bacterial lipopolysaccharide, J. Endotoxin Res. 6 (2000) 489–491.
[22] A.B. Schromm, E. Lien, P. Henneke, J.C. Chow, A. Yoshimura, H. Heine, E. Latz, B.G. Monks, D.A. Schwartz, K. Miyake, D.T. Golenbock, Molecular genetic analysis of an endotoxin nonresponder mutant cell line: a point mutation in a conserved region of MD-2 abolishes endotoxin-induced signaling, J. Exp. Med. 194 (2001) 79–88.
[23] J. da Silva Correia, K. Soldau, U. Christen, P.S. Tobias, R.J. Ulevitch, Lipopolysaccharide is in close proximity to each of the proteins in its membrane receptor complex. transfer from CD14 to TLR4 and MD-2, J. Biol. Chem. 276 (2001) 21129–21135.
[24] Y. Nagai, S. Akashi, M. Nagafuku, M. Ogata, Y. Iwakura, S. Akira, T. Kitamura, A. Kosugi, M. Kimoto, K. Miyake, Essential role of MD-2 in LPS responsiveness and TLR4 distribution, Nat. Immunol. 3 (2002) 667–672.
[25] O. Takeuchi, K. Hoshino, T. Kawai, H. Sanjo, H. Takada, T. Ogawa, K. Takeda, S. Akira, Differential roles of TLR2 and TLR4 in recognition of gram-negative and gram-positive bacterial cell wall components, Immunity 11 (1999) 443–451.
[26] A.E. Medvedev, K.M. Kopydlowski, S.N. Vogel, Inhibition of lipopolysaccharide-induced signal transduction in endotoxin-tolerized mouse macrophages: dysregulation of cytokine, chemokine, and toll-like receptor 2 and 4 gene expression, J. Immunol. 164 (2000) 5564–5574.
[27] T. Nakano, T. Sonoda, C. Hayashi, A. Yamatodani, Y. Kanayama, T. Yamamura, H. Asai, T. Yonezawa, Y. Kitamura, S.J. Galli, Fate of bone marrow-derived cultured mast cells after intracutaneous, intraperitoneal, and intravenous transfer into genetically mast cell-deficient W/Wv mice. Evidence that cultured mast cells can give rise to both connective tissue type and mucosal mast cells, J. Exp. Med. 162 (1985) 1025–1043.
[28] M. Tsai, R.H. Chen, S.Y. Tam, J. Blenis, S.J. Galli, Activation of MAP kinases, pp90rsk and pp70-S6 kinases in mouse mast cells by signaling through the c-kit receptor tyrosine kinase or Fc epsilon RI: rapamycin inhibits activation of pp70-S6 kinase and proliferation in mouse mast cells, Eur. J. Immunol. 23 (1993) 3286–3291.
[29] S. Akashi, R. Shimazu, H. Ogata, Y. Nagai, K. Takeda, M. Kimoto, K. Miyake, Cutting edge: cell surface expression and lipopolysaccharide signaling via the toll-like receptor 4-MD-2 complex on mouse peritoneal macrophages, J. Immunol. 164 (2000) 3471–3475.
[30] M. Muroi, T. Ohnishi, K. Tanamoto, Regions of the mouse CD14 molecule required for toll-like receptor 2- and 4-mediated activation of NF-kappa B, J. Biol. Chem. 277 (2002) 42372–42379.
[31] F. Randow, B. Seed, Endoplasmic reticulum chaperone gp96 is required for innate immunity but not cell viability, Nat. Cell Biol. 3 (2001) 891–896.
[32] M.W. Hornef, B.H. Normark, A. Vandewalle, S. Normark, Intracellular recognition of lipopolysaccharide by toll-like receptor 4 in intestinal epithelial cells, J. Exp. Med. 198 (2003) 1225–1235.
[33] A. Visintin, A. Mazzoni, J.A. Spitzer, D.M. Segal, Secreted MD-2 is a large polymeric protein that efficiently confers lipopolysaccharide sensitivity to Toll-like receptor 4, Proc. Natl. Acad. Sci. USA 98 (2001) 12156–12161.
[34] F. Re, J.L. Strominger, Monomeric recombinant MD-2 binds toll-like receptor 4 tightly and confers lipopolysaccharide responsiveness, J. Biol. Chem. 277 (2002) 23427–23432.
[35] R. Dziarski, Q. Wang, K. Miyake, C.J. Kirschning, D. Gupta, MD-2 enables Toll-like receptor 2 (TLR2)-mediated responses to lipopolysaccharide and enhances TLR2-mediated responses to Gram-positive and Gram-negative bacteria and their cell wall components, J. Immunol. 166 (2001) 1938–1944.
[36] K. Kawasaki, S. Akashi, R. Shimazu, T. Yoshida, K. Miyake, M. Nishijima, Mouse toll-like receptor 4.MD-2 complex mediates lipopolysaccharide-mimetic signal transduction by Taxol, J. Biol. Chem. 275 (2000) 2251–2254.

[37] Y. Bulut, E. Faure, L. Thomas, H. Karahashi, K.S. Michelsen, O. Equils, S.G. Morrison, R.P. Morrison, M. Arditi, Chlamydial heat shock protein 60 activates macrophages and endothelial cells through Toll-like receptor 4 and MD2 in a MyD88-dependent pathway, J. Immunol. 168 (2002) 1435–1440.

[38] Y. Okamura, M. Watari, E.S. Jerud, D.W. Young, S.T. Ishizaka, J. Rose, J.C. Chow, J.F. Strauss III, The extra domain A of fibronectin activates Toll-like receptor 4, J. Biol. Chem. 276 (2001) 10229–10233.

[39] R. Malaviya, Z. Gao, K. Thankavel, P.A. van derMerwe, S.N. Abraham, The mast cell tumor necrosis factor alpha response to FimH-expressing *Escherichia coli* is mediated by the glycosylphosphatidylinositol-anchored molecule CD48, Proc. Natl. Acad. Sci. USA 96 (1999) 8110–8115.

[40] A.P. Prodeus, X. Zhou, M. Maurer, S.J. Galli, M.C. Carroll, Impaired mast cell-dependent natural immunity in complement C3-deficient mice, Nature 390 (1997) 172–175.

Dual Role of Fcγ Receptor in Transient Focal Cerebral Ischemia in Mice

Miki Komine-Kobayashi, MD; Nei Chou, MD; Hideki Mochizuki, MD; Atsuhito Nakao, MD; Yoshikuni Mizuno, MD; Takao Urabe, MD

Background and Purpose—Cerebral ischemia/reperfusion injury is associated with the development of inflammatory response, including pathological contributions by vascular leukocytes and endogenous microglia. Expression of Fc receptors (FcRs) on macrophages and microglia is thought to be involved in the inflammatory cascade. The present study assessed the role of FcγR in ischemia/reperfusion injury, using FcγR knockout ($Fc\gamma R^{-/-}$) mice and bone marrow chimera $Fc\gamma R^{-/-}$ mice, which express enhanced green fluorescent protein (EGFP).

Methods—Mice underwent occlusion of the middle cerebral artery for 60 minutes, followed by reperfusion. Infarct volume and mortality were calculated at several time points after ischemia. To clarify the function and distribution of microglia/macrophages, immunohistochemical staining and immunoblotting of ionized calcium-binding adapter molecule 1 (Iba-1), inducible nitric oxide synthase, and nitrotyrosine were performed.

Results—$Fc\gamma R^{-/-}$ mice showed significantly reduced mortality (20%) and smaller infarcts (19.7±3.63 versus 33.28±7.98 mm^3; $P<0.001$) than wild-type (WT) mice at 72 hours after reperfusion. Western blotting revealed that microglial activation ($P<0.002$) and induction of inducible nitric oxide synthase ($P<0.005$) were reduced in $Fc\gamma R^{-/-}$ mice compared with WT mice. At 7 days after reperfusion, sections double-immunostained for EGFP and Iba-1 showed less activation and migration of EGFP-positive bone marrow–derived macrophages in $Fc\gamma R^{-/-}$ chimera mice than in WT mice.

Conclusions—Our results demonstrated that the neuroprotective effect of FcγR deficiency in our model may be primarily attributed to the suppression of activation and infiltration of inflammatory cells. (***Stroke.*** **2004;35:958-963.)**

Key Words: microglia ■ macrophages ■ Fc-gamma receptor ■ inflammation ■ ischemia/reperfusion injury

The inflammatory response in the central nervous system is considered important in the pathological process after the onset of cerebral ischemia and is a risk factor for the initial development of cerebral ischemia.[1] Brain ischemia induces a marked response of resident microglia and hematopoietic cells, including monocytes and macrophages, and elicits a strong intrinsic inflammatory response involving activation of microglia, recruitment of granulocytes, and infiltration of macrophages in the ischemic area.[2] However, whether the molecular mechanisms underlying these inflammatory responses are beneficial or detrimental in cerebral infarction is still unclear. Understanding the intracellular signaling mechanism and cell-to-cell interaction in the inflammatory cascade may help in the design of therapeutic strategies for cerebral infarction.

Recent studies have emphasized the critical roles of Fc receptors (FcRs) expressed on macrophages and microglia in the inflammatory cascade.[3,4] Although several studies stressed the importance of the FcγR in the inflammatory response in immunological[5] and degenerative diseases[6] of the central nervous system, to our knowledge no report has described a link between FcγR and cerebral ischemia.

In a previous study we provided direct evidence for the migration and distribution of bone marrow–derived monocytes/macrophages and the relationship between resident microglia and infiltrated hematogenous elements in the ischemic brain of bone marrow chimera mice that expressed enhanced green fluorescent protein (EGFP).[7] It is conceivable that microglia/macrophages may serve a dual and paradoxical role after ischemic injury. To assess the role of Fcγ receptor in ischemia/reperfusion injury, middle cerebral artery (MCA) occlusion/reperfusion was performed in the FcγR knockout ($Fc\gamma R^{-/-}$) mice and the bone marrow chimera $Fc\gamma R^{-/-}$ mice with the use of a model system established previously.

Materials and Methods

Transient Focal Cerebral Ischemia

The protocol described here received prior approval by the Committee on Animal Experimental Guidelines of Juntendo University School of Medicine. $Fc\gamma R^{-/-}$ mice (Jackson Laboratory) were generated by the homogeneous recombination method, as described previously.[8] Studies were conducted in 8-week-old $Fc\gamma R^{-/-}$ and C57BL/6 (wild-type [WT]) (n=50 per group) mice of the same

Received September 22, 3003; final revision received December 2, 2003; accepted December 17, 2003.

From the Department of Neurology (M.K.-K., N.C., H.M., Y.M. T.U.), Research Institute for Old Age (H.M., Y.H.), Juntendo University School of Medicine, Tokyo, and Department of Immunology (A.N.), University of Yamanashi Faculty of Medicine, Yamanashi, Japan.

Correspondence to Takao Urabe, MD, Department of Neurology, Juntendo University School of Medicine, 2-1-1 Hongo, Bunkyo-ku, Tokyo 113-0033, Japan. E-mail t_urabe@med.juntendo.ac.jp

Stroke is available at http://www.strokeaha.org

DOI: 10.1161/01.STR.0000120321.30916.8E

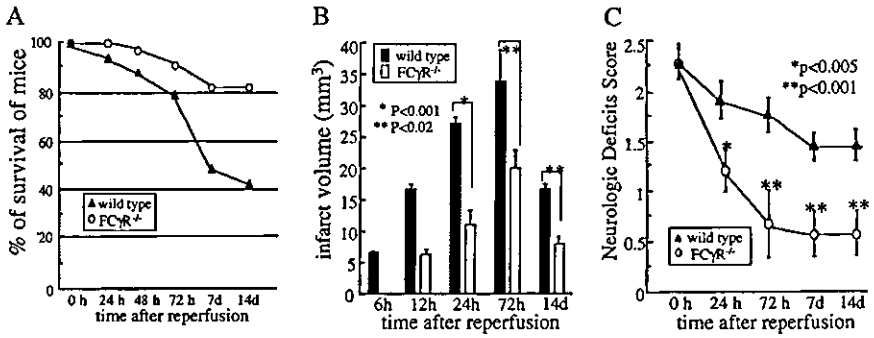

Figure 1. A, Survival analysis during 14 days after reperfusion in WT and FcγR$^{-/-}$ mice. B, Effects of FcγR depletion on stroke outcome. Infarct volume was compared among FcγR$^{-/-}$ mice and WT littermates at different time points after reperfusion. C, Neurological deficit scores in WT and FcγR$^{-/-}$ mice at different time points after reperfusion.

genetic background. Animals were housed under diurnal lighting and provided with food and water ad libitum.

Mutant and WT mice, weighing 20 to 25 g, were initially anesthetized with 4.0% isoflurane and maintained on 1.0% to 1.5% isoflurane in 70% N_2O and 30% O_2 with the use of a small-animal anesthesia system. The tip of the laser-Doppler probe was placed on the area selected for regional cerebral blood flow monitoring, which corresponded to the territory of the occluded MCA. The left MCA was occluded for 60 minutes and then reperfused as described previously.[9] In another group of mice (n=10), reperfusion was not performed (permanent MCA occlusion group). Body temperature was kept at 37°C during the experiment with a heating pad. We generated the FcγR$^{-/-}$/EGFP transgenic model by bone marrow transplantation of EGFP into FcγR$^{-/-}$ mice, using the method reported previously,[7] and induced transient cerebral ischemia in these animals 6 weeks later.

Estimation of Infarct Volume

At 6, 12, 24, or 72 hours or 14 days after reperfusion, the mice were anesthetized by intraperitoneal injection of 50 mg/kg pentobarbital (n=5 per group) and decapitated. The brains were coronally sectioned into six 1-mm-thick slices. The slices were incubated for 20 minutes in 2% solution of 2,3,5-triphenyltetrazolium chloride at 37°C and immersion-fixed in 4% buffered formalin solution. To compensate for brain edema, the correct infarct volume was calculated as described in detail previously.[10]

Neurological Evaluation

Neurological examination was performed daily after reperfusion until the animals were killed. The observer was blinded to the study protocol and scored the postural reflexes using a modified neurological scoring system described previously.[9] In this system, score 0 represents no observable neurological deficits; 1, failure to extend the left forepaw on lifting the whole body by the tail; 2, circling to the contralateral side; and 3, loss of walking or righting reflex.

Immunohistochemistry

Five animals of each group were anesthetized by intraperitoneal injection of pentobarbital (50 mg/kg) at 12, 24, and 72 hours and 7 and 14 days after reperfusion. The brain was removed immediately and postfixed for 24 hours in 4% paraformaldehyde in PBS at 4°C before cryoprotection by bathing in 30% sucrose. It was then frozen, and 20-μm-thick consecutive coronal sections were prepared on a cryostat (CM-1900, Leica). Immunohistochemical staining was performed for CD64, ionized calcium-binding adapter molecule 1 (Iba-1; a kind gift from Dr Kohsaka[11]), and inducible nitric oxide synthase (iNOS, BD Bioscience). Sections were washed in PBS, incubated in 0.3% H_2O_2 in PBS for 30 minutes, and incubated overnight at 4°C with 10% normal goat serum (Dako Corporation) in PBS and anti-Iba-1 (1:1500) antibody, anti-iNOS (1:300) antibody, or anti-CD64 (1:300) antibody. Immunoreactivity was visualized by the avidin-biotin complex method (Vectastatin, Vector Laboratories) as described previously.[7]

Double-Immunofluorescence Staining

Free-floating sections of EGFP bone marrow chimera mouse were washed with PBS and incubated in a blocking solution, 3% Block-Ace (Yukijirushi) in T-PBS (0.5% Triton X-100), for 30 minutes at room temperature. Double-immunofluorescence staining was performed by simultaneous incubation of sections with anti–Iba-1 antibody, anti-iNOS antibody, or anti-nitrotyrosine antibody (1:50; Upstate Biotechnology) overnight 4°C. For double labeling, the primary antibodies were detected with Texas red–conjugated secondary antibody (1:500; Vector Laboratories) afterward for 2 hours at room temperature. The sections were washed with PBS and mounted on microslide glass with Vectorshield Mounting Medium (Vector Laboratories).

Western Blots

Four animals of each group were decapitated after 24 or 72 hours of reperfusion. Samples were taken from 2 regions: the ischemic region and the contralateral cortex. Protein extraction and Western blotting were performed.[11] Aliquots containing 50 μg of protein were subjected to 10% sodium dodecyl sulfate–polyacrylamide gel electrophoresis. Protein bands were transferred to nitrocellulose membranes (Amersham Pharmacia Biotech) with the use of an electrophoretic transfer system (Trans-blot Semi-dry Transfer Cell, Bio-Rad). After they were blocked with BlockAce for 1 hour, the membranes were incubated overnight at 4°C with anti–Iba-1 antibody (1:5000), anti-iNOS antibody (1:1000), or anti–α-tubulin antibody (1:1000; Santa Cruz Biotechnology Inc). After incubation with the appropriate horseradish peroxidase–conjugated secondary antibody (1:25 000; Amersham) for 1 hour at room temperature, immunoreactive bands were visualized in the linear range with enhanced chemiluminescence (ECL Western blotting system, (Amersham). For quantitative evaluation, the immunoreactive bands were subjected to densitometric analysis.

Cell Count and Statistical Analysis

In each coronal section of Iba-1 staining, the numbers of Iba-1–positive cells at the transition area were counted independently by 2 investigators. Values presented in this study are expressed as mean±SD. After acquisition of all data, the randomization code was broken, and the data were assigned to the respective group. One-way ANOVA and subsequent post hoc Fisher protected least significant difference test were used to determine the statistical significance of differences in physiological variables, neurological score, and volume of infarction between the 2 groups.

Results

Effects of FcγR Deficiency on Transient Focal Cerebral Ischemia

Figure 1A shows that the survival rate of FcγR$^{-/-}$ mice (80%) was significantly increased 14 days after reperfusion compared with WT mice. In the permanent MCA occlusion group, 10% of WT mice and 50% of FcγR$^{-/-}$ mice died with signs of brain swelling and herniation within 24 hours (data not shown). At 24

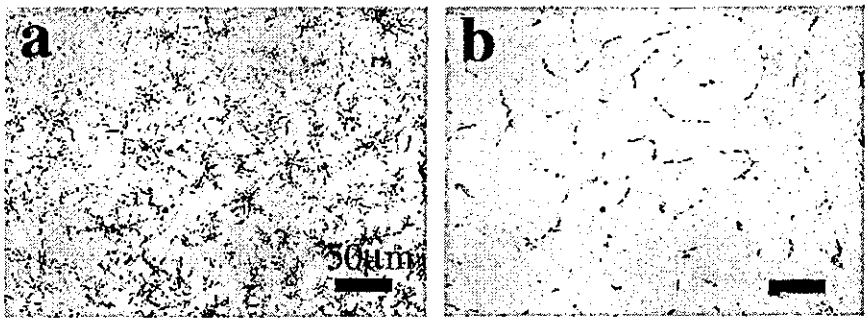

Figure 2. Photographs show FcγRI (CD64) immunostaining in untreated WT and FcγR$^{-/-}$ mice. a, FcγR immunostaining was observed in many glial cells with microglial morphology in the cortex of WT mice. b, However, there was no specific FcγR immunostaining in FcγR$^{-/-}$ mice. Magnification ×200.

hours after reperfusion, the infarct size (10.89±1.26 mm^3) in FcγR$^{-/-}$ mice was significantly smaller (P<0.001) than that in WT littermates (26.59±1.26 mm^3) (Figure 1B). After 72 hours of reperfusion, the infarct size was 19.7±3.63 mm^3 in FcγR$^{-/-}$ mice and 33.28±7.98 mm^3 in WT littermates. The neurological deficit scores are shown in Figure 1C. The scores of FcγR$^{-/-}$ mice recorded at several time points after reperfusion were significantly lower (P<0.005) than those of WT mice.

Microglial Activation in FcγR$^{-/-}$ Mice After Ischemia/Reperfusion

FcγRI immunostaining was detected in glial cells, which morphologically resembled microglia (Figure 2a). However, no specific FcγRI immunostaining was noted in the brain of FcγR$^{-/-}$ mice (Figure 2b).

The distribution of infarct area was analyzed with the use of cresyl violet–stained sections. We defined each ischemic lesion by location in 3 areas (ischemic core, transition area, and peri-infarct area), as shown schematically in Figure 3Aa as areas C, B, and A, respectively. In WT mice, activation of microglia was identified by Iba-1 antibody in the peri-infarct and transition areas. Ramified Iba-1–positive microglia were detected in the ischemic core at 12 hours after reperfusion (Figure 3Aa). Such microglial activation was widely distributed and gradually increased in the peri-infarct and transition areas until 7 days after MCA reperfusion and then tended to decrease (Figure 3Aa to 3Af). On the other hand, the microglial response was less evident in the ischemic core in a time-dependent manner. In FcγR$^{-/-}$ mice, microglial activity in the transition area was weak (Figure 3Ag to 3Al)

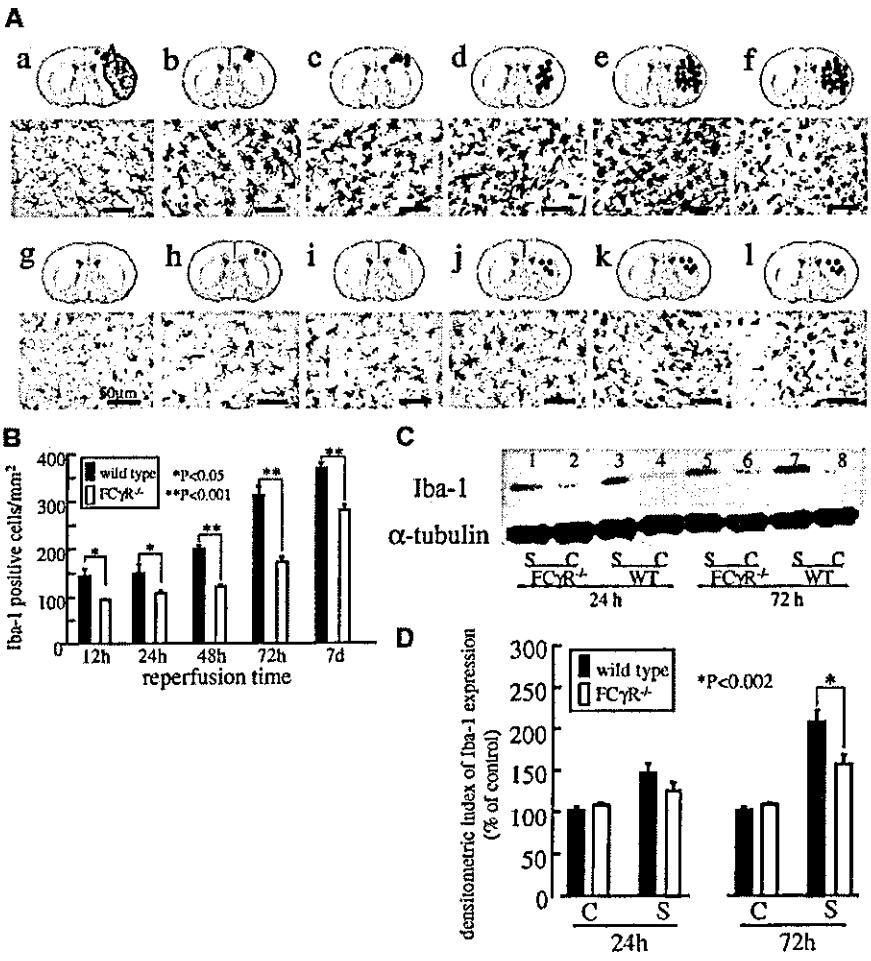

Figure 3. A, Schematic representation of distribution of neuronal damage in mouse brain after reperfusion. Shaded area represents the infarct zone (a). Three areas subjected to immunohistochemical analysis are illustrated: A, peri-infarct area; B, transition area; C, ischemic core area. Photographs show Iba-1 immunostaining in the transition area of representative WT (a to f) and FcγR$^{-/-}$ (g to l) mice. Shown are 12 hours (a, g), 24 hours (b, h), 48 hours (c, i), 72 hours (d, j), 7 days (e, k), and 14 days (f, l) after reperfusion. Dots on the brain schema represent the distribution of Iba-1–immunoreactive cells. Magnification ×200. B, Numbers of Iba-1–positive microglia at different time points. C, Western blot analysis. Samples were prepared from the brain at 24 hours (FcγR$^{-/-}$ mice: lanes 1 and 2; WT mice: lanes 3 and 4) and 72 hours (FcγR$^{-/-}$ mice: lanes 5 and 6; WT mice: 7 and 8) after reperfusion. A 17-kDa band corresponding to Iba-1 protein was clearly detected in the ischemic lesion, and the intensity of the band increased in the stroke side in a time-dependent manner. A weaker band was noted in FcγR$^{-/-}$ mice than in WT littermates. D, Densitometric analysis. Values are expressed as percentage of control. C indicates contralateral lesion; S, stroke side.

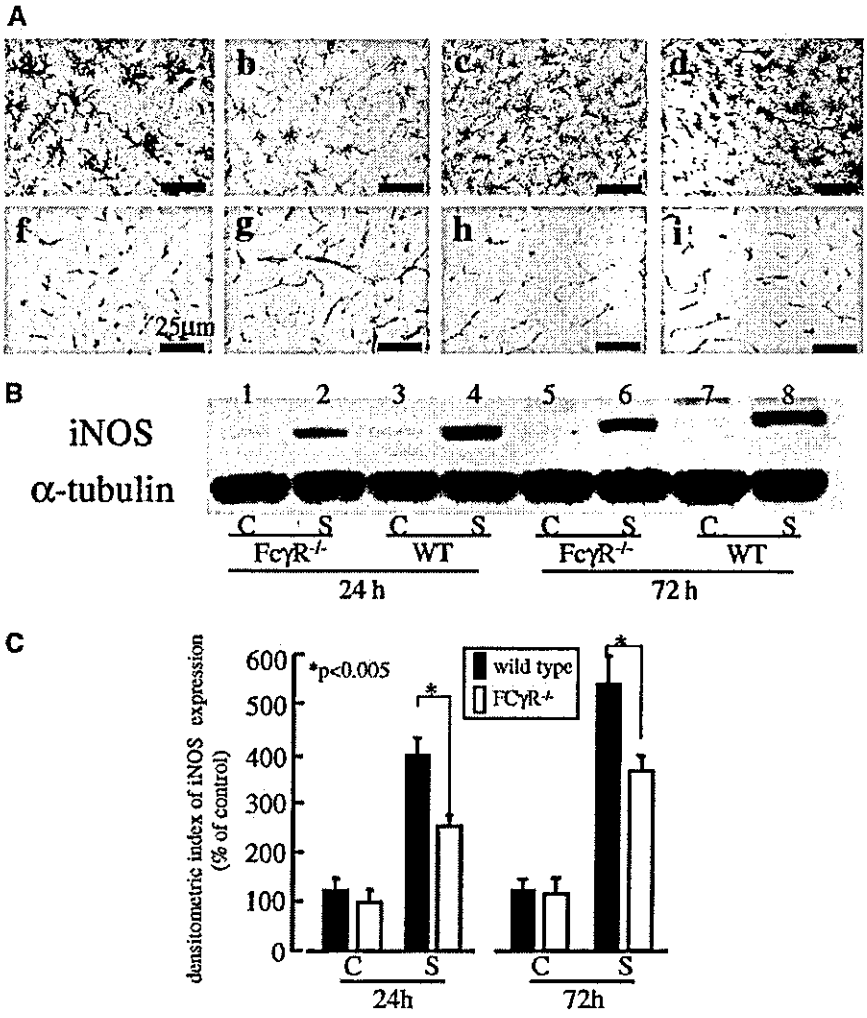

Figure 4. A, Photomicrographs show iNOS staining in representative WT and $Fc\gamma R^{-/-}$ mice. Shown are WT mice (a to d) and $Fc\gamma R^{-/-}$ mice (e to h) 24 hours (a, e), 48 hours (b, f), 72 hours (c, g), and 7 days (d, h) after reperfusion. In WT mice, many iNOS-positive cells were detected in microglia in the transition area, while iNOS immunoreactivity was observed only in the endothelial cells in the ischemic core of $Fc\gamma R^{-/-}$ mice. Magnification ×200. B, Western blot analysis of iNOS. The samples were prepared from the brain at 24 hours ($Fc\gamma R^{-/-}$ mice: lanes 1 and 2; WT mice: lanes 3 and 4) and 72 hours ($Fc\gamma R^{-/-}$ mice: lanes 5 and 6; WT mice: lanes 7 and 8) after reperfusion. With the use of iNOS antibody, a 130-kDa band was detected on the stroke side. The intensity of the specific band increased in a time-dependent manner. $Fc\gamma R^{-/-}$ mice showed less intensity of the band. C, Densitometric analysis. Values are expressed as percentage of control. C indicates contralateral lesion; S, stroke side.

compared with WT mice (Figure 3Aa to 3Af, 3B). Immunoblots of Iba-1 were clearly detected in the ischemic lesion as a protein band at 17 kDa. In WT mice, the intensity of the band increased in the stroke side ($P<0.002$) in a time-dependent manner compared with $Fc\gamma R^{-/-}$ mice (Figure 3C, 3D).

Induction of iNOS in $Fc\gamma R^{-/-}$ Mice

In WT mice, induction of iNOS in microglia of the peri-ischemic area reached a peak level at 48 to 72 hours after reperfusion (Figure 4Ab, 4Ac). On the other hand, in $Fc\gamma R^{-/-}$ mice, iNOS was detected only in endothelial cells of the ischemic core area (Figure 4Ae to 4Ah). Immunoblots of iNOS were detected as a protein band at 130 kDa. In WT mice, the intensity of the iNOS band in the stroke side was stronger ($P<0.005$) than the corresponding site in $Fc\gamma R^{-/-}$ littermates (Figure 4B, 4C).

Activation of Bone Marrow–Derived Macrophages in $Fc\gamma R^{-/-}$ Mice

At 7 days after reperfusion, double immunostaining for EGFP and Iba-1 showed many morphologically phagocytic EGFP/Iba-1–positive cells in the ischemic core and many amoeboid-like EGFP/Iba-1–positive cells in the transition area of WT/EGFP chimera mice. These findings indicated activation and migration of EGFP-positive bone marrow–derived microglia/macrophages in WT/EGFP chimera mice (Figure 5b, 5c). In contrast, microglial staining was comparatively less in $Fc\gamma R^{-/-}$/EGFP chimera mice (Figure 5e, 5f), and only a few ramified Iba-1/EGFP–positive cells with branching processes were detected in the transitional area. In WT/EGFP chimera mice, some EGFP/iNOS-positive cells were detected in the transition area, but many EGFP-positive intrinsic microglia did not exhibit iNOS and were observed in endothelial cells (Figure 5g, 5h). On the other hand, iNOS staining was detected only in endothelial cells in the $Fc\gamma R^{-/-}$/EGFP chimera mice (data not shown). In WT/EGFP chimera mice, induction of nitrotyrosine in microglia of the transition area was detected (Figure 5i), and nitrotyrosine staining was observed in the luminal surface of vessels at ischemic lesions (Figure 5j), while there were few nitrotyrosine-positive cells in $Fc\gamma R^{-/-}$/EGFP chimera mice (data not shown). These nitrotyrosine-positive microglia did not stain for EGFP.

Discussion

In the present study we analyzed the effects of brain ischemia on the functional contribution of FcγR by using $Fc\gamma R^{-/-}$ mice. The major finding of the present study was that $Fc\gamma R^{-/-}$ mice were protected from progression and expansion of infarct volume after focal cerebral ischemia followed by reperfusion.

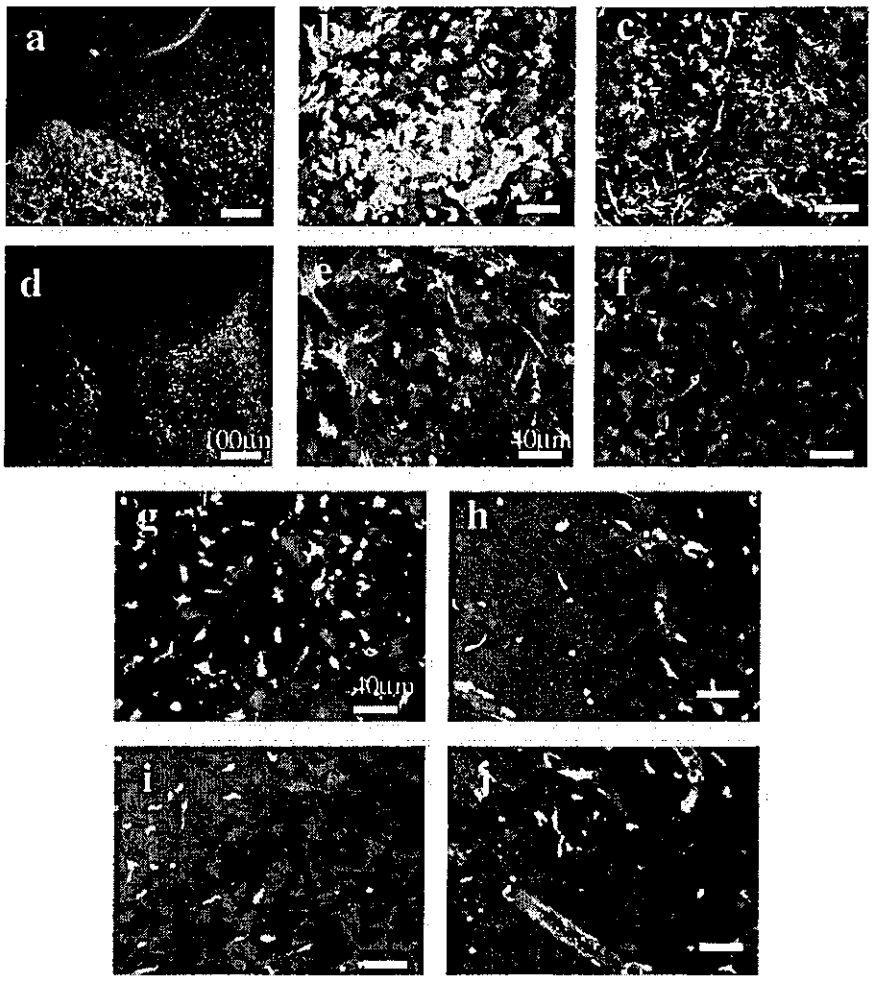

Figure 5. Photomicrographs show double-immunofluorescence labeling of WT/EGFP (a to c, g to j) and FcγR$^{-/-}$/EGFP chimera mouse (d to f) brain. Shown are 7 days (a to f) and 72 hours (g to j) after reperfusion at the ischemic core (b, e) and transition area (c, f to j). a to f, Iba-1–stained cells appear red in color. EGFP/Iba-1–positive cells are seen in these areas. Many irregularly shaped EGFP/Iba-1–positive cells and some with processes are seen in WT/EGFP chimera mice (a to c), while fewer cells are detected in FcγR$^{-/-}$/EGFP littermates (d to f). g, h, iNOS/EGFP double-immunofluorescence staining of WT/EGFP chimera mouse. i, j, Nitrotyrosine/EGFP double-immunofluorescence staining of WT/EGFP chimera mouse. Magnification ×100 for a and d; magnification ×400 for b, c, e to j.

To our knowledge, there are no studies that proposed the involvement of a FcγR-dependent pathway in the pathogenesis of cerebral ischemia/reperfusion injury. FcγR promotes phagocytosis, antibody-dependent cell-mediated cytotoxicity, activation of inflammatory cells, and antibody-dependent immunity.[12] In the present study, using FcγR$^{-/-}$ mice, we demonstrated that FcγR contributed to the activation of microglia, induction of iNOS followed by generation of reactive oxygen species, and infiltration of bone marrow–derived macrophages during cerebral ischemia/reperfusion. To our knowledge, this is the first report on the functional role of FcγR on microglia/macrophages in cerebral ischemia/reperfusion injury.

Cerebral ischemia/reperfusion injury is associated with the development of inflammatory response, including pathological contributions from vascular leukocytes and endogenous microglia.[2] In the ischemic brain, microglia/macrophages are the major source of inflammatory cytokines.[1,13] Therefore, inhibition of microglial activation can protect against stroke-associated pathological changes.[14] After ischemia, microglial activation results in a series of functional and morphological modifications that involve proliferation.[15] The present results showed that microglial activation was markedly suppressed in ischemic lesions from the early stage of reperfusion in FcγR$^{-/-}$ mice compared with WT mice. Our results provide strong evidence that FcγR plays a crucial role in the initiation and progression of neuronal damage by activation and proliferation of microglia.

In WT mice, iNOS immunoreactivity was observed in activated microglia and reached a peak level at 48 to 72 hours after reperfusion. However, in FcγR$^{-/-}$ mice, iNOS immunoreactivity was not detected in microglia but only in endothelial cells. In addition, iNOS-positive microglia and nitrotyrosine-positive microglia were observed in WT/EGFP chimera mice but not in FcγR$^{-/-}$/EGFP littermates. In our bone marrow transplantation model, induction of iNOS does not occur on the invading macrophages. Therefore, the possible mechanisms involved in the reduction of infarction volume during brain ischemia/reperfusion include the suppression of activation of microglia followed by induction of iNOS and peroxynitrite production through the FcγR-dependent pathway. In contrast to neuronal NOS, which generates NO early after onset of ischemia,[16] iNOS appears somewhat later in inflammatory cells and contributes to the evolution of brain injury. Furthermore, suppression of iNOS expression has been demonstrated to play a major role as a protective agent in several experimental models, such as iNOS null mice,[16,17] treatment with antisense oligodeoxynucleotide to iNOS,[18] administration of iNOS inhibitors,[19] and mild hypothermia.[20] In the present study, therefore, it is possible that the potential neuroprotective role of the FcγR-dependent pathway is mediated in part by the suppression of

iNOS upregulation and peroxynitrite production in activated microglia.

In our bone marrow transplantation model, although FcγR was present in the donor EGFP-positive cells, activation and migration of EGFP-positive bone marrow–derived macrophages were markedly reduced in FcγR$^{-/-}$ mice compared with WT mice. Microglial activation has been observed as early as 6 hours after insult,[21] followed by subsequent macrophage transmigration. A previous study reported that reactive microglia showed increased expression of FcRs and that engagement of FcγR triggered inflammatory, cytolytic, or phagocytic activities.[22] The mechanism of migration and infiltration of bone marrow–derived cells into infarcted areas is a topic of debate and remains unclear but may involve the FcγR-dependent pathway for macrophages or some activating signals from activated microglia. Taken together, our results indicate that the signaling pathway through the FcγR on residual microglia may play an important role in the migration and activation of bone marrow–derived macrophages.

In this study we demonstrated that FcγR deficiency decreased the inflammatory responses through microglial activation, iNOS induction, and bone marrow–derived macrophage infiltration after transient focal cerebral ischemia/reperfusion. Therefore, the neuroprotective effect of FcγR deficiency may be primarily attributable to suppression of inflammatory cell activation and infiltration. Our data showed that anti-inflammatory therapy through the FcγR may be useful for neuroprotection after cerebral infarction. Suppression of the FcγR-dependent pathway may provide an approach to potentially reduce ongoing damage during reperfusion in stroke patients.

Acknowledgments

This study was supported in part by a High Technology Research Center grant and a grant-in-aid for exploratory research from the Ministry of Education, Culture, Sports, Science, and Technology, Japan. The anti–Iba-1 polyclonal antibody was a kind gift from Y. Imai and S. Kohsaka from the Department of Neurochemistry, National Institute of Neuroscience, Tokyo, Japan.

References

1. Davies CA, Loddick SA, Toulmond S, Stroemer RP, Hunt J, Rothwell NJ. The progression and topographic distribution of interleukin-1beta expression after permanent middle cerebral artery occlusion in the rat. *J Cereb Blood Flow Metab.* 1999;19:87–98.
2. Clark RK, Lee EV, White RF, Jonak ZL, Feuerstein GZ, Barone FC. Reperfusion following focal stroke hastens inflammation and resolution of ischemic injured tissue. *Brain Res Bull.* 1994;35:387–392.
3. Ravetch JV. Fc receptors: rubor redux. *Cell.* 1994;78:553–560.
4. Sylvestre DL, Ravetch JV. Fc receptors initiate the Arthus reaction: redefining the inflammatory cascade. *Science.* 1994;265:1095–1098.
5. Abdul-Majid K-B, Stefferl A, Bourquin C, Lassmann H, Linington C, Olsson T, Kleinau S, Harris RA. Fc receptors are critical for autoimmune inflammatory damage to the central nervous system in experimental autoimmune encephalomyelitis. *Scand J Immunol.* 2002;55:70–81.
6. He Y, Le WD, Appel SH. Role of Fc receptors in nigral cell injury induced by Parkinson disease immunoglobulin injection into mouse substantia nigra. *Exp Neurol.* 2002;176:322–327.
7. Tanaka R, Komine-Kobayashi M, Mochizuki M, Yamada M, Furuya T, Migita M, Shimada T, Mizuno Y, Urabe T. Migration of enhanced green fluorescent protein expressing bone marrow-derived microglia/macrophage into the mouse brain following permanent focal ischemia. *Neuroscience.* 2003;117:531–539.
8. Suzuki Y, Shirato I, Okumura K, Ravetch JV, Takai T, Tomino Y, Ra C. Distinct contribution of Fc receptors and angiotensin II-dependent pathways in anti-GBM glomerulonephritis. *Kidney Int.* 1998;54:1166–1174.
9. Hara H, Huang PL, Panahian N, Fishman MC, Moskowitz MA. Reduced brain edema and infarction volume in mice lacking the neuronal isoform of nitric oxide synthase after transient MCA occlusion. *J Cereb Blood Flow Metab.* 1996;16:605–611.
10. Lin TN, He YY, Wu G, Khan M, Hsu CY. Effect of brain edema on infarct volume in a focal cerebral ischemia model in rats. *Stroke.* 1993;24:117–121.
11. Ito D, Imai Y, Ohsawa K, Nakajima K, Fukuuchi Y, Kohsaka S. Microglia-specific localisation of a novel calcium binding protein, Iba1. *Mol Brain Res.* 1998;57:1–9.
12. Ravetch JV, Kinet JP. Fc receptors. *Annu Rev Immunol.* 1991;9:457–492.
13. Lambertsen K, Gregersen R, Finsen B. Microglial-macrophage synthesis of tumor necrosis factor after focal cerebral ischemia in mice is strain dependent. *J Cereb Blood Flow Metab.* 2000;20:53–65.
14. Yrjanheikki J, Tikka T, Keinanen R, Goldsteins G, Chan PH, Koistinaho J. A tetracycline derivative, minocycline, reduces inflammation and protects against focal cerebral ischemia with a wide therapeutic window. *Proc Natl Acad Sci U S A.* 1999;96:13496–13500.
15. Kato H. The role of microglia in ischemic brain injury. In: Feurstein GZ, ed. *Inflammation and Stroke.* Boston: Birkhauser Verlag, 2001;89–99.
16. Iadecola C. Bright and dark sides of nitric oxide in ischemic brain injury. *Trends Neurosci.* 1997;20:132–139.
17. Zhao X, Haensel C, Araki E, Ross ME, Iadecola C. Gene-dosing effect and persistence of reduction in ischemic brain injury in mice lacking inducible nitric oxide synthase. *Brain Res.* 2000;872:215–218.
18. Parmentier-Batteur S, Bohme GA, Lerouet D, Zhou-Ding L, Beray V, Margaill I, Plotkine M. Antisense oligodeoxynucleotide to inducible nitric oxide synthase protects against transient focal cerebral ischemia-induced brain injury. *J Cereb Blood Flow Metab.* 2001;21:15–21.
19. Nagayama M, Zhang F, Iadecola C. Delayed treatment with aminoguanidine decreases focal cerebral ischemic damage and enhances neurological recovery in rats. *J Cereb Blood Flow Metab.* 1998;18:1107–1113.
20. Han HS, Qiao Y, Karabiyikoglu M, Giffard RG, Yenari MA. Influence of mild hypothermia on inducible nitric oxide synthase expression and reactive nitrogen production in experimental stroke and inflammation. *J Neurosci.* 2002;22:3921–3928.
21. Lyons SA, Pastor A, Ohlemeyer C, Kann O, Wiegand F, Prass K, Knapp F, Kettenmann H, Dirnagl U. Distinct physiologic properties of microglia and blood-borne cells in rat brain slices after permanent middle cerebral artery occlusion. *J Cereb Blood Flow Metab.* 2000;20:1537–1549.
22. Ulvestad E, Williams K, Vedeler C, Antel J, Nyland H, Mϕrk M, Matre R. Reactive microglia in multiple sclerosis lesions have an increased expression of receptors for the Fc part of IgG. *J Neurol Sci.* 1994;121:125–131.

Journal of Dermatological Science (2004) 34, 54–55

ELSEVIER

Journal of Dermatological SCIENCE

www.intl.elsevierhealth.com/journals/jods

LETTER TO THE EDITOR

Expression of phosphorylated Smad2 in normal human epidermis

Transforming growth factor-β (TGF-β) is a multifunctional cytokine that plays an important role in the regulation of cell growth, differentiation, apoptosis, and extracellular matrix production in a variety of cell types [1]. In the skin, abundant expression of three mammalian isoforms of TGF-βs (TGF-β1, -β2, -β3) are demonstrated at mRNA and protein levels in human epidermis by using in situ hybridization technique or immunohistochemistry [2–4] and it has been implicated in growth regulation of keratinocytes based on the evidence that (1) TGF-βs inhibit proliferation of normal human keratinocytes in vitro [5] and (2) transgenic mice that overexpress dominant negative TGF-β type II receptor in the epidermis show hyperplastic epidermis with increased BrdU uptake in basal and suprabasal keratinocytes [6].

However, elucidating functional significance of TGF-β expression in the skin has been hampered by the fact that TGF-β is produced and secreted by cells in a latent form, which must then be activated before interaction with TGF-β receptors on the cell surface [7]. Mere elevation of TGF-β mRNA or protein expression is therefore not automatically an indication that active TGF-β is being produced. Thus, even though several papers reported TGF-β mRNA or protein expression in normal and pathological states of human epidermis, it might not be an accurate reflection of active TGF-β secretion in the human epidermis.

Therefore, to determine whether human epidermis indeed received signals of TGF-β, we examined expression of phosphorylated Smad2 in normal human skin by immunohistochemical study using an antibody specifically recognized phosphorylated Smad2. Recent studies have revealed that TGF-β1, -β2, -β3 bind to the cell surface TGF-β type I and type II receptors and the ligand-bound activated TGF-β receptor complex phosphorylate cytoplasmic Smad2 and Smad3, which form hetero-trimeric complex with Smad4, respectively, and enter the nucleus, bind directly or indirectly to DNA, and regulate transcription of many TGF-β target genes in cooperation with various transcriptional factors [8]. Thus, phosphorylation of Smad2 or Smad3 is a key event for initiation of TGF-β signalling.

Normal skin samples were obtained from subjects undergoing plastic surgery ($n = 6$) after written informed consent. As shown in Fig. 1, we found that expression of phosphorylated Smad2 was prominent in the nucleus of keratinocytes in whole epidermis of the skin specimen. Similar finding was observed in all the normal skin specimens from six subjects. The exclusive nuclear staining of phosphorylated Smad2 indicated that Smad2 was activated by TGF-β receptors and translocated to the nucleus in keratinocytes. Thus, the data suggested that normal human epidermis received signals of TGF-β in vivo.

As a comparison, we performed tunnel staining in normal human epidermis because terminal differentiation of normal human keratinocytes might be associated with enhanced cellular TGF-β and apoptotic cell death [9]. We asked whether phosphorylated Smad2-positive cells were parallel with keratinocytes undergoing apoptosis. As shown in Fig. 2, TUNEL positive cells in the epidermis were largely detected at the granular layer in the epidermis, which was different from the expression pattern of phosphorylated Smad2. The results may suggest that activation of TGF-β/Smad2 signalling is not relevant to induction of keratinocyte apoptosis in vivo because phosphorylation of Smad2 is observed in basal and suprabasal keratinocytes which are not committed to apoptosis. However, of course, more thorough investigation is required to prove that activation of TGF-β/Smad2 signalling is not involved in apoptotic cell death in human epidermis.

In conclusion, human epidermis receives signals of TGF-β, that is constitutively synthesised by epidermal keratinocytes as shown by many previous reports. It should be determined in future whether signalling pathways downstream of TGF-β/Smad2 is active or not and what physiological functions the TGF-β/Smad2 pathway mediates in human epidermis. Most importantly, how Smad2 activation occurs (how conversion of latent form of TGF-β to its active form occurs) in normal human epidermis remains to be elucidated.

0923-1811/$30.00
doi:10.1016/j.jdermsci.2003.10.004

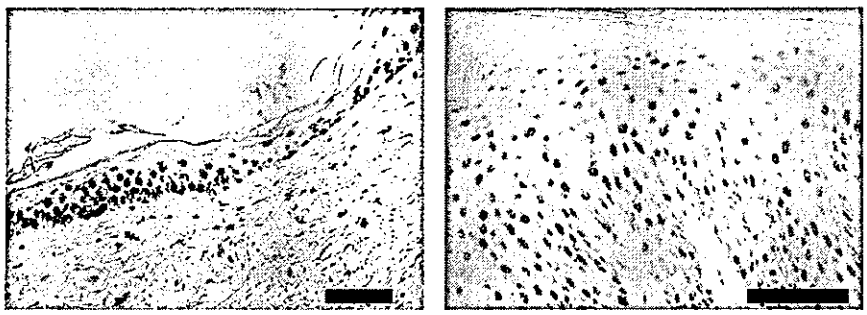

Fig. 1 Expression of phosphorylated Smad2 in normal human epidermis. Four micrometer of cryostat sections of normal skin samples obtained from subjects undergoing plastic surgery were incubated with rabbit polyclonal antibody against phosphorylated Smad2 (#3101, Cell Signaling Technology Inc., Beverly, MA, USA) and then incubated with a biotinylated goat anti-rabbit antibody (1/200). Sections were then incubated with avidin biotin peroxidase complex (1/500) and 3-amino-9-ethyl carbazole (Sigma) was used as chromogen. Between steps, the slides were rinsed in Tris-buffered saline with 0.1% Triton X-100. All sections were lightly counterstained with hematoxylin. Positive cells were stained as brown in the nucleus. Scale bars represent 50 μm.

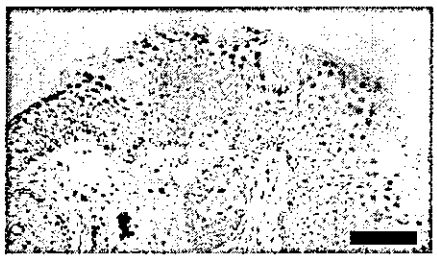

Fig. 2 TUNEL staining in normal human epidermis. In situ detection of DNA fragmentation of the skin specimens obtained as described above was performed using terminal deoxynucleotidyltransferase-mediated dUTP nick-end labeling (TUNEL) staining using in situ tunnel staining kit (Takara Corp., Japan) according to the manufacturer's recommendation. Positive cells were stained as brown in the nucleus. Scale bars represent 50 μm.

References

[1] Roberts AB, Sporn MB. Physiological actions and clinical applications of transforming growth factor-beta (TGF-beta). Growth Factors 1993;8:1–9.

[2] Kane CJ, Knapp AM, Mansbridge JN, Hanawalt PC. Transforming growth factor-beta 1 localization in normal and psoriatic epidermal keratinocytes in situ. J Cell Physiol 1990;144:144–50.

[3] Schmid P, Cox D, Bilbe G, McMaster G, Morrison C, Stahelin H, et al. TGF-betas and TGF-beta type II receptor in human epidermis: differential expression in acute and chronic skin wounds. J Pathol 1993;171:191–7.

[4] Quan T, He TY, John SK, Voorhees JJ, Fisher GJ. Ultraviolet irradiation alters transforming growth factor-β/Smad pathway in human skin in vivo. J Invest Dermatol 2002;119:499–506.

[5] Moses HL, Yang EY, Pietenpol JA. Regulation of epithelial proliferation by TGF-β. Ciba Found Symp 1991;157:66–74.

[6] Wang XJ, Greenhalgh DA, Bickenbach JR, Jiang A, Bundman DS, Krieg T, et al. Expression of a dominant-negative type II transforming growth factor beta (TGF-beta) receptor in the epidermis of transgenic mice blocks TGF-beta-mediated growth inhibition. Proc Natl Acad Sci USA 1997;94:2386–91.

[7] Miyazono K, Hellman U, Wernstedt C, Heldin CH. Latent high molecular weight complex of transforming growth factor-β. J Biol Chem 1988;263:6407–15.

[8] Massague J. How cells read TGF-β signals. Nature Rev Mol Cell Biol 2000;1:169–78.

[9] Min BM, Woo KM, Lee G, Park NH. Terminal differentiation of normal human oral keratinocytes is associated with enhanced cellular TGF-β and phospholipase C-γ1 levels and apoptotic cell death. Exp Cell Res 1999;249:377–85.

Meethong Prapars
Atsuhito Nakao*
Nobuhiro Nakano
Long Jin
Hideoki Ogawa
Department of Dermatology, Atopy Research Center, Juntendo University School of Medicine 2-1-1 Hongo, Bunkyo-ku, Tokyo 113-8421, Japan
*Corresponding author. Present address Department of Immunology, Faculty of Medicine University of Yamanashi, 1110 Shimokato, Tamaho Yamanashi 409-3898, Japan
Tel.: +81-55-273-6752; fax: +81-55-273-9542
E-mail address: anakao@yamanashi.ac.jp
(A. Nakao)

Microbiol. Immunol., 48(10), 755–759, 2004

Genotype Analysis of *Malassezia restricta* as the Major Cutaneous Flora in Patients with Atopic Dermatitis and Healthy Subjects

Takashi Sugita*[,1], Mami Tajima[2], Misato Amaya[2], Ryoji Tsuboi[2], and Akemi Nishikawa[3]

[1]*Department of Microbiology and* [3]*Department of Immunobiology, Meiji Pharmaceutical University, Kiyose, Tokyo 204–8588, Japan, and* [2]*Department of Dermatology, Tokyo Medical University, Shinjuku-ku, Tokyo 160–0023, Japan*

Received May 18, 2004; in revised form, June 29, 2004. Accepted July 6, 2004

***Abstract*: Lipophilic yeasts of the genus *Malassezia* colonize the skin surface of humans and are an exacerbating factor in atopic dermatitis (AD). Two species, *M. restricta* and *M. globosa* are major cutaneous microflora in both AD patients and healthy subjects. We compared the DNA sequences of the intergenic spacer (IGS) region, located between the 26S and 5S rRNA genes of *M. restricta* colonizing the skin surfaces of 13 AD patients and 12 healthy subjects, and of three CBS stock strains as references. The IGS 1 sequences were divided into two major groups, corresponding to AD patients and healthy subjects. These findings suggest that a specific genotype of *M. restricta* plays a significant role in AD, although *M. restricta* commonly colonizes both AD patients and healthy subjects.**

***Key words*: *Malassezia restricta*, Atopic dermatitis, Cutaneous microflora, Genotype, IGS**

Lipophilic yeasts in the genus *Malassezia* are part of the normal human cutaneous microflora and are isolated from sebaceous-rich areas, particularly the chest, back, and head. They are a causative factor in *pityriasis versicolor* and seborrheic dermatitis (1, 4). In addition, *Malassezia* species are also thought to exacerbate atopic dermatitis (AD), based on findings that AD patients have specific serum IgE antibodies to *Malassezia* (11, 21, 22). Application of topical antifungal agents by AD patients decreases *Malassezia* colonization and the severity of eczematous lesions (2), suggesting that *Malassezia* species play a role in AD. We have analyzed the cutaneous *Malassezia* microflora of AD patients and healthy subjects using a non-culture method (nested PCR) (16). While *M. restricta* and *M. globosa* were detected in approximately 90% of the AD patients, other *Malassezia* species were found in fewer than 40%. In addition, we analyzed the DNA sequence divergence of the IGS region, which is located between the 26S and 5S rRNA genes of *M. globosa*, and found that the IGS sequence of *M. globosa* from AD patients differed from that from healthy subjects (19). These findings suggest that a specific genotype of this microorganism plays a significant role in AD.

**Address correspondence to* Dr. Takashi Sugita, Department of Microbiology, Meiji Pharmaceutical University, 2–522–1 Noshio, Kiyose, Tokyo 204–8588, Japan. Fax: +81–424–95–8762. E-mail: sugita@my-pharm.ac.jp

This paper describes the genotype of one of the major *Malassezia* microflora species, *M. restricta*, obtained from the skin of AD patients and healthy subjects.

Materials and Methods

Direct DNA sequencing of the IGS 1 region of M. restricta *stock strains.* Three stock strains obtained from the Centraalbureau voor Schimmelcultures (Utrecht, The Netherlands) were analyzed: CBS 7877 (type strain of *M. restricta*), CBS 7991, and CBS 8747. The first two were isolated from the skin of a healthy subject in the UK, and the third was from the scalp of a healthy subject in Canada (http://www.cbs.knaw.nl/). Genomic DNA was extracted using the method of Makimura et al. (12). The IGS region containing 5S rDNA was amplified from each strain using the primer pair 26SBF (5'-AGCTGCTGCCAATGCTAGCTC) and Mala-R (5'-TACTGCTGTGAATGCTCCAGC) (18). The PCR products were sequenced using an ABI 310 DNA sequencer and a BigDye Terminator Cycle Sequencing Ready Reaction kit version 3.1 (Perkin-Elmer Applied Biosystems, Calif., U.S.A.) according to the manufacturer's instructions.

Abbreviations: AD, atopic dermatitis; CBS, Centraalbureau voor Schimmelcultures; IGS, intergenic spacer.

Subjects. Thirteen AD outpatients (9 males, 4 females; aged 20 to 64 years, mean age 33.9±11.3 years) at Tokyo Medical University Hospital and 12 healthy students (3 males, 9 females; aged 19 to 23 years, mean age 20.7±1.5 years) at Meiji Pharmaceutical University were involved in this study. AD was diagnosed according to the criteria of Hanifin and Rajka (6), and samples were collected from erythematous lesions on the face and neck. Routine skin care, including intermittent applications of mild steroid ointment or petrolatum, was administered before sampling. Written informed consent was obtained from each subject.

Sequencing IGS 1 region from samples. Malassezia samples were collected by applying transparent OpSite dressing (Smith and Nephew Medical, Ltd., Hull, U.K.), and fungal DNA was extracted from the OpSite dressing as described previously (16). The species-specific primer pair: Res-IGS-1F (5'-CGACCTAGTCGACTACATCCTAC) and Res-IGS-1R (5'-ATGAGGAGGAAAGGCAGGCAAG) were designed from the IGS 1 sequence analysis. The DNA pellet was resuspended in 30 μl of TE (10-mM Tris-HCl [pH 8.0], 1-mM EDTA [pH 8.0]). The DNA extracted (10 μl) from each sample was added to 40 μl of PCR master mixture, which consisted of 5 μl of 10× PCR buffer (TaKaRa), 4 μl of 200-μM deoxynucleoside triphosphates, 10 pmol of each primer, and 0.5 U of TaKaRa Ex *Taq* DNA polymerase (TaKaRa). PCR was performed with an initial denaturation at 94 C for 1 min, followed by 30 cycles of 30 sec at 94 C, 1 min at 54 C, and 30 sec at 72 C, and a final extension at 72 C for 10 min. The PCR products were cloned using a TA Cloning Kit (Invitrogen Corp., Calif., U.S.A.) and three positive clones were sequenced.

Molecular phylogenetic analysis. The sequences of the IGS 1 region obtained from the samples of AD patients and healthy subjects were aligned using Clustal W (20). For neighbor-joining analysis (13), the distances between sequences were calculated using Kimura's two-parameter model (8). A bootstrap analysis was conducted with 100 replications (5).

Formation of chimeric molecules. To confirm whether chimeric molecules formed under the PCR conditions used in this study, mixed genomic DNA from known *Malassezia* species (*M. dermatis, M. furfur, M. globosa, M. japonica, M. obtusa, M. slooffiae, M. sympodialis, M. pachydermatis*, and *M. yamatoensis*) was used for PCR co-amplification of the IGS region. Then, the IGS amplified from the mixed genomes was cloned; 30 clones were selected at random, and their sequences were determined.

Results

IGS 1 Sequence Analysis of M. restricta

Stock strains. Complete sequences of the IGS 1 region were determined for three CBS stock strains of *M. restricta*. Their sizes ranged from 620 to 661 bp. *M. restricta* IGS 1 had two short sequence repeats (SSR) of (CA)n and (CT)n at positions 125–134 and 178–189 in the IGS sequence of strain CBS7877 (type strain), respectively. The nucleotide sequences determined in this study have been deposited with the DNA Data Bank of Japan (DDBJ) under accession numbers AB178809 (CBS7877), AB178808 (CBS7991), and AB178810 (CBS8747).

Samples from subjects. Before the IGS sequence analysis of the samples, formation of chimeric molecules was investigated. Thirty clones were chosen at random and sequenced; none were identified as a chimeric molecule. Using the PCR conditions described above, 454- to 515-bp fragments were partially amplified and analyzed. A phylogenetic tree was constructed from 28 IGS 1 sequences obtained from the samples of 13 AD patients, 12 healthy subjects, and three CBS stock strains (Fig. 1). The tree consisted of two major groups separated with 100% bootstrap support. Group 1 included 10 AD patients and three CBS stock strains, and Group 2 contained all 12 healthy subjects and three AD patients. The IGS 1 sequences derived from the AD patients (Group 1) were more diverse than those from the healthy subjects (Group 2). An alignment of the partial sequences of representative strains from Groups 1 and 2 is shown in Fig. 2. The sequence similarity between the two groups was below 70%. Two SSRs, (CA)n and (CT)n, were also found in the IGS 1 sequence from each sample. For both SSRs, there were more sequence repeats in the IGS 1 region of samples from the healthy subjects than from AD patients: (CA)n, AD patients, 6.8±3.9 repeats; healthy subjects, 14.7±1.2 repeats; (CT)n, AD patients, 6.8±2.0 repeats; healthy subjects, 9.7±1.9 repeats.

Discussion

We have described differences in the IGS 1 genotypes of *M. restricta* colonizing the skin surfaces of AD patients and healthy subjects. rRNA gene sequences have been used for molecular phylogeny, taxonomy, and identification (10, 14). Of the subunits or regions in this gene, the IGS region shows remarkable intraspecies diversity. We have reported the analytical significance of the IGS region using *Cryptococcus neoformans* and *Trichosporon asahii* (15, 17). *M. globosa*, which is a

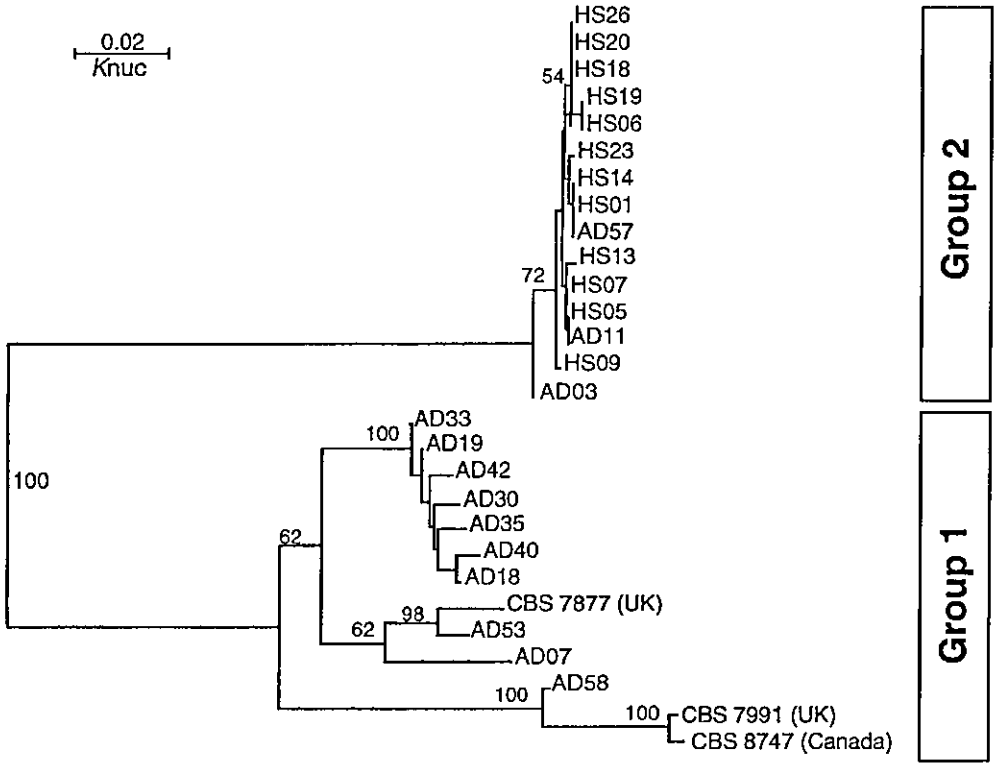

Fig. 1. Phylogenetic tree of *M. restricta* colonizing the skin surfaces of AD patients and healthy subjects based on DNA sequences of the IGS 1 region. AD, patient with atopic dermatitis; HS, healthy subject. The numbers are the confidence levels from 100 replicate bootstrap samplings (frequencies less than 50% are not shown). K_{nc}, Kimura's parameter (8).

```
AD33        1 CGACCTAGTCGACTACATCCTACTGTATCCTACGCAATGGAGGTGTGTATGGTAGGTCAC
HS01        1 CGACCTAGTCGACTACATCCTACTGTATTCTACGCAATGGAGGTGTGTATTGTAGGACAC
              *************************** ********************** ***** ***

AD33       61 ATCCTACCCCACTTTCCCATTCTTCTATACCTTACCCCCCTACCCCCTCTCTACGTCACC
HS01       61 AT-----------------------------------------ACACCCACCCCACAT-A--
              **                                          ** *** * * ** * *

AD33      121 CGTGCACACACACA--------------------TTCACGCCTGTCTATGCGTCCCCCTC
HS01       79 ----CACACACACACACACACACACACACACACAGTCGTCACCC----------------
                  **********                    **     *

AD33      161 CTCCAAGAGTCGAATTTCTCTCTCTCTCT----------CGTCAGTCTACTTGCCCATGG
HS01      119 -----------------CTCTCTCTCTCTCTCTCTCTCTCGTCAGTCTACTTGGCCATGT
                               ************          ************** *****
```

Fig. 2. Alignment of the DNA sequences of the IGS 1 regions of representative sequences. AD, patient with atopic dermatitis; HS, healthy subject. The SSRs are underlined: (CA)n and (CT)n.

major cutaneous microflora, also has four genotypes (19). Of the four genotypes, two groups were found in AD patients; one group was from healthy subjects, and the other included samples from both AD patients and healthy subjects. This suggests that a specific genotype of *M. globosa* plays a significant role in AD. The present study also indicates that the IGS genotype of *M. restricta* obtained from AD patients is different from

that of healthy subjects. Three CBS stock strains were included in this study as reference strains; although they were isolated from healthy subjects, they are located in the AD cluster in the tree (Fig. 1). The CBS strains were from British or Canadian subjects. It is still not known whether our finding is specific for the Japanese population, or the CBS strains are an exception. This requires further analysis of *M. restricta* strains from other countries. The *M. restricta* IGS, like that of *M. globosa*, also has SSRs that could be used to distinguish microorganisms present in AD patients and healthy individuals.

The reason for the difference in the genotypes found in each population is unclear, but might reflect selection against *M. restricta* strains. There are three possible causes: (1) the effect of skin surface lipids, (2) the effect of ointments or cream bases, or (3) antifungal drug susceptibility. The main skin surface lipids are triglycerides, squalene, wax esters, cholesterol, ceramides, and free fatty acids (3). Although the lipid composition in AD patients is generally not different from that of healthy subjects, a significant decrease in ceramide 1 and differences in the concentrations of the related linoleate and oleate molecules have been reported (7, 24). Such differences in composition might affect colonization by *Malassezia* strains with different lipid requirements. The base ingredient of an ointment or cream can affect the growth of microorganisms, as with the growth of *M. furfur, M. globosa*, and *M. sympodialis* (9), but effects on *M. restricta* are unknown. Antifungal drug susceptibility might be responsible for selection of strains. A correlation between antifungal susceptibility and genotype has been reported in *Candida albicans* (23). However, because no patient in this study received antifungal therapy, this possibility can be excluded.

In conclusion, our IGS sequence analysis showed that the genotypes of *M. restricta* colonizing the skin surface of AD patients and healthy subjects are significantly different. Therefore, genotype should be considered when studying the relationship between *M. restricta* and AD.

This study was supported in part by Research Grant C (16590127) from the Japan Society for the Promotion of Science (TS).

References

1) Ashbee, H.R., and Evans, E.G. 2002. Immunology of diseases associated with *Malassezia* species. Clin. Microbiol. Rev. **15**: 21–57.
2) Back, O., Scheynius, A., and Johansson, S.G. 1995. Ketoconazole in atopic dermatitis: therapeutic response is correlated with decrease in serum IgE. Arch. Dermatol. Res. **287**: 448–451.
3) Downing, D.T., Stewart, M.E., and Strauss, J.S. 1999. Lipids of the epidermis and the sebaceous glands, p. 144–155. *In* Freedberg, I.M., Eisen, A.Z., Wolff, K., Austen, K.F., Goldsmith, L.A., Katz, S.I., and Fitzpatrick, T.B. (eds), Fitzpatrick's dermatology in general medicine, 5th ed, McGraw-Hill, N.Y.
4) Faergemann, J. 2002. Atopic dermatitis and fungi. Clin. Microbiol. Rev. **15**: 545–563.
5) Felsenstein, J. 1985. Confidence limits on phylogenies: an approach using the bootstrap. Evolution **39**: 783–791.
6) Hanifin, J.M., and Rajka, G. 1980. Diagnostic features of atopic dermatitis. Acta Derm. Venereol. **92**: 4–47.
7) Hara, J., Higuchi, K., Okamoto, R., Kawashima, M., and Imokawa, G. 2000. High-expression of sphingomyelin deacylase is an important determinant of ceramide deficiency leading to barrier disruption in atopic dermatitis. J. Invest. Dermatol. **115**: 406–413.
8) Kimura, M. 1980. A simple method for estimation evolutionary rate of base substitutions through comparative studies of nucleotide sequences. J. Mol. Evol. **16**: 111–120.
9) Koyama, T., Kanbe, T., Kikuchi, A., and Tomita, Y. 2002. Effects of topical vehicles on growth of the lipophilic *Malassezia* species. J. Dermatol. Sci. **29**: 166–170.
10) Kurtzman, C.P., and Robnett, C.J. 1997. Identification of clinically important ascomycetous yeasts based on nucleotide divergence in the 5' end of the large-subunit (26S) ribosomal DNA gene. J. Clin. Microbiol. **35**: 1216–1223.
11) Leung, D.Y. 1995. Atopic dermatitis: the skin as a window into the pathogenesis of chronic allergic diseases. J. Allergy Clin. Immunol. **96**: 302–318.
12) Makimura, K., Murayama, Y.S., and Yamaguchi, H. 1994. Detection of a wide range of medically important fungal species by polymerase chain reaction (PCR). J. Med. Microbiol. **40**: 358–364.
13) Saitou, N., and Nei, M. 1987. The neighbor-joining method: a new method for reconstructing phylogenetic trees. Mol. Biol. Evol. **4**: 406–425.
14) Sugita, T., Nishikawa, A., Ikeda, R., and Shinoda, T. 1999. Identification of medically relevant *Trichosporon* species based on sequences of internal transcribed spacer regions and construction of a database for *Trichosporon* identification. J. Clin. Microbiol. **37**: 1985–1993.
15) Sugita, T., Ikeda, R., and Shinoda, T. 2001. Diversity among strains of *Cryptococcus neoformans* var. *gattii* as revealed by a sequence analysis of multiple genes and a chemotype analysis of capsular polysaccharide. Microbiol. Immunol. **45**: 757–768.
16) Sugita, T., Suto, H., Unno, T., Tsuboi, R., Ogawa, H., Shinoda, T., and Nishikawa, A. 2001. Molecular analysis of *Malassezia* microflora on the skin of atopic dermatitis patients and healthy subjects. J. Clin. Microbiol. **39**: 3486–3490.
17) Sugita, T., Nakajima, M., Ikeda, R., Matsushima, T., and Shinoda, T. 2002. Sequence analysis of the ribosomal DNA intergenic spacer 1 regions of *Trichosporon* species. J. Clin.